Faculty of Science, Medicine & Health - Honours Theses

University of Wollongong Thesis Collections

2021

Monitoring of CO2 Fluxes from Differing Vegetation Communities using the Eddy Covariance Approach

Matthew Spann

Follow this and additional works at: https://ro.uow.edu.au/thsci

Recommended Citation

Monitoring of CO2 Fluxes from Differing Vegetation Communities using the Eddy Covariance Approach

Abstract

Coastal vegetated ecosystems, including wetlands and saltmarsh, have been widely recognised as providing a range of environmental, social, and cultural benefits. They have the ability to store more carbon than nearly any other vegetated system, making them the target of increasing study due to the potential play a role in the mitigation of some effects of climate change. Wetland vegetation have been recognised for having a high carbon sequestration rate. But the carbon cycling dynamics between vegetation types in Australian saltmarshes is lesser known. Framed within a small wetland on the New South Wales South Coast, this research project aimed to monitor greenhouse gas fluxes and how environmental variables influence these fluxes. Monitoring was carried out through the erection of two eddy covariance flux towers which measure fluxes of CO_2 from the wetland surface. Soil and water sampling was conducted to analyse salinity, bulk density, carbon content and pH, while measuring biomass across vegetation communities. Using these measurements, expected differences in fluxes between two vegetation communities with differing vegetation structures and compositions were identified. These two communities were differentiated by their dominant species, one by Sarcocornia quinqueflora, and the other by Juncus kraussii. The comparison of the two communities allowed for potential drivers of CO_2 fluxes to be identified, based on the sampled environmental variables, and their location within the wider wetland itself. Fluxes of CO_2 differed between the two monitored vegetation communities. This difference occurred when comparing both the 24-hour average of half-hourly flux data and the daytime-only half-hourly average flux data. The Juncus-dominated community had a stronger negative CO_2 flux than the Sarcocornia-dominated community, indicating a stronger ability to drawn down more carbon out of the atmosphere (-0.078 ± 0.013 and -0.029 ± 0.0063 mg CO_2 m-2 s-1 respectively). The possibility of a freshwater lens occurring beneath the Juncus community was identified as being a potential driver between the differing CO_2 fluxes, as this would subsequently control the salinity and productivity of the community. Biomass was higher in the Juncus community, with an average biomass of 1.40 kg m2, and soil salinity in this community was lower than the Sarcocornia community on both sampling occasions. iii It was also found that the monitored wetland was acting as a net sink for CO_2 using the two measured vegetation communities. However, it is important to consider that this project only measured atmospheric fluxes and is missing information on lateral exchanges of carbon within the groundwater. Further sampling and monitoring of fluxes and environmental variables are recommended to form a more complete picture of the driving forces of CO_2 fluxes in this wetland. It is also recommended to monitor methane fluxes from the wetland, as this would allow for a more holistic few of the carbon exchanges within the wetland. So, while the Lake Tilba salt marsh site is relatively small, monitoring here could provide a starting point for predicting how fluxes of CO_2 are influenced within wetlands along the NSW South Coast.

Degree Type
Thesis

Degree Name
Bachelor of Environmental Science (Honours)

Department
School of Earth, Atmospheric and Life Sciences

Advisor(s)
Jeffrey Kelleway

Monitoring of CO_2 Fluxes from Differing Vegetation Communities using the Eddy Covariance Approach

Matthew Spann

Supervisors:

Dr Jeffrey Kelleway, Dr Nicholas Deutscher, Dr Michael Hughes

This thesis is presented as part of the requirement for the conferral of the degree:

Bachelor of Environmental Science (Honours)

University of Wollongong

School of Earth and Environmental Science

October 2021

1. Abstract

Coastal vegetated ecosystems, including wetlands and saltmarsh, have been widely recognised as providing a range of environmental, social, and cultural benefits. They have the ability to store more carbon than nearly any other vegetated system, making them the target of increasing study due to the potential play a role in the mitigation of some effects of climate change. Wetland vegetation have been recognised for having a high carbon sequestration rate. But the carbon cycling dynamics between vegetation types in Australian saltmarshes is lesser known. Framed within a small wetland on the New South Wales South Coast, this research project aimed to monitor greenhouse gas fluxes and how environmental variables influence these fluxes. Monitoring was carried out through the erection of two eddy covariance flux towers which measure fluxes of CO_2 from the wetland surface. Soil and water sampling was conducted to analyse salinity, bulk density, carbon content and pH, while measuring biomass across vegetation communities.

Using these measurements, expected differences in fluxes between two vegetation communities with differing vegetation structures and compositions were identified. These two communities were differentiated by their dominant species, one by *Sarcocornia quinqueflora*, and the other by *Juncus kraussii.* The comparison of the two communities allowed for potential drivers of CO_2 fluxes to be identified, based on the sampled environmental variables, and their location within the wider wetland itself.

Fluxes of CO_2 differed between the two monitored vegetation communities. This difference occurred when comparing both the 24-hour average of half-hourly flux data and the daytime-only half-hourly average flux data. The Juncus-dominated community had a stronger negative CO_2 flux than the Sarcocornia-dominated community, indicating a stronger ability to drawn down more carbon out of the atmosphere (-0.078 ± 0.013 and -0.029 ± 0.0063 mg CO_2 m^{-2} s^{-1} respectively). The possibility of a freshwater lens occurring beneath the Juncus community was identified as being a potential driver between the differing CO_2 fluxes, as this would subsequently control the salinity and productivity of the community. Biomass was higher in the Juncus community, with an average biomass of 1.40 kg m^2, and soil salinity in this community was lower than the Sarcocornia community on both sampling occasions.

It was also found that the monitored wetland was acting as a net sink for CO_2 using the two measured vegetation communities. However, it is important to consider that this project only measured atmospheric fluxes and is missing information on lateral exchanges of carbon within the groundwater. Further sampling and monitoring of fluxes and environmental variables are recommended to form a more complete picture of the driving forces of CO_2 fluxes in this wetland. It is also recommended to monitor methane fluxes from the wetland, as this would allow for a more holistic few of the carbon exchanges within the wetland. So, while the Lake Tilba salt marsh site is relatively small, monitoring here could provide a starting point for predicting how fluxes of CO_2 are influenced within wetlands along the NSW South Coast.

Acknowledgments

Covid Impact Statement:

Due to the impact of the stay-at-home orders enforced by the NSW Government as a result of the June Coronavirus Outbreak, sample analysis in the lab was put on hold until appropriate Covid-Safe guidelines could be put in place. Hence, lab time was limited until after this was put in place. As mentioned throughout this Thesis, the Health Orders also restricted return trips to the study site for data downloads and subsequent sample collection. This reduced the temporal resolution of data available for analysis. Because of this, no seasonal trends in fluxes or environmental parameters were able to be discerned. Despite these challenges, I was still able to complete and submit the report by the required due data.

Certification

I, Matthew Spann, declare that this thesis submitted in fulfilment of the requirements for the conferral of the degree Bachelor of Environmental Science (Honours), from the University of Wollongong, is wholly my own work unless otherwise referenced or acknowledged. This document has not been submitted for qualifications at any other academic institution.

Matthew Spann

14th October 2021)

List of Abbreviations:

IPCC	Intergovernmental Panel on Climate Change
DPIE	Department of Planning Industry and Environment
GHG	Greenhouse Gases
CO_2	Carbon Dioxide
H_2O	Water
CH_4	Methane
N_2O	Nitrous Oxide
N_2	Nitrogen
$\%C_{org}$	Percent organic carbon
Tg	Teragram
Mg	Megagram
µg	Microgram
ha	Hectare
EbA	Ecosystem-based Adaptation
ICOLL	Intermittently Closed and Open Lakes and Lagoon
NEE	Net Ecosystem Exchange
GEP	Gross Ecosystem Production
R_{eco}	Ecosystem Respiration
VOC	Volatile Organic Compounds
BD	Bulk Density
DBD	Dry Bulk Density
EC	Eddy Covariance

Table of Contents

List of Figures:

List of Tables

2. Introduction

Coastal vegetated ecosystems, like tidal salt marshes, are known to provide varied societal benefits - they are places of high biodiversity, and provide habitat for economically valued species and protection to coastal communities from storm surge and subsequent erosion (Hyndes *et al.*, 2014; Luo *et al.*, 2019; Rosentreter *et al.*, 2021). However, perhaps the most important benefit these ecosystems may offer, is their ability to sequester more carbon than nearly any other vegetated ecosystem (Saintilan *et al.*, 2013; Abdul-Aziz *et al.*, 2018; Byrd *et al.*, 2018; Rogers *et al.*, 2019; Rosentreter *et al.*, 2021). Carbon stored in these coastal ecosystems is referred to as 'blue carbon', and it is this coastal nature that allows such high amounts of carbon to be sequestered. Unlike their terrestrial counterparts, soils in coastal salt marshes are exposed to anaerobic conditions on a regular basis, lowering the ability of microbes in the soil to oxidise organic material and release the carbon back into the atmosphere as carbon dioxide (CO_2) (Rosentreter *et al.*, 2021).

The ability to sequester carbon makes coastal vegetated ecosystems the target of increasing study, as they have the potential to remove CO_2 from the atmosphere and store it in sediments, acting in a way that has the potential to mitigate some effects of climate change. Thus, these ecosystems also provide opportunities for governments to include their carbon sequestration capacities in National Determined Contributions under the Paris Agreement (Rosentreter *et al.*, 2021). Two avenues are then opened-up for policy, one that focuses on preservation of existing coastal ecosystems, less existing carbon stores be released back into the atmosphere as CO_2, and secondly, restoration of depleted or degraded coastal ecosystems (Rosentreter *et al.*, 2021). The importance offered to both government policy and the international fight against climate change means that these coastal ecosystems and how they interact with their surrounding environments must be better understood. The research undertaken within this project aims to delineate interactions between hydrology, salinity, soil properties and vegetation, and how these affect the variation of blue carbon within an ecosystem, and the subsequent influence on greenhouse gas fluxes.

The research will be framed within a coastal wetland at Tilba Tilba Lake on the South Coast of New South Wales, Australia, and was conducted from February to October 2021. The overarching aims of the research are as follows:

- Firstly, to monitor greenhouse gas fluxes from the wetland surface – which includes vegetation – to determine if there is a difference between vegetation communities.
- Secondly, to assess how the particular environmental parameters mentioned above influence gas fluxes, and
- Finally, to examine how these environmental parameters, including soil carbon vary across the wetland.

It is hypothesised that:

- There will be a significant different between the CO_2 fluxes of the Sarcocornia and Juncus vegetation communities, and
- Differences in CO_2 fluxes between communities may be driven by biomass, salinity or inundation regimes.

3. Literature Review:

3.1. Coastal Wetlands in Australia

Saltmarshes cover over 13000 square kilometres of Australia's coastline (Department of the Environment and Energy, 2016). This coverage is after an estimated 25 percent decline in overall saltmarsh throughout Australian estuaries since 1950. Some estuaries have been estimated to have lost up to 80 percent of their saltmarsh coverage, which has led to saltmarsh communities being listed as a vulnerable community under the Australian Commonwealth *Environment Protection and Biodiversity Conservation Act 1999* (Department of the Environment and Energy, 2016). Additionally, in New South Wales, coastal saltmarsh is listed as an Endangered Ecological Community under the *NSW Biodiversity Conservation Act 2016*. (NSW Government, 2021). Saltmarsh presence provides a range of social, cultural and environmental benefits. They support a diverse range of species, from economically and recreationally important fish and invertebrates, insects and molluscs to migratory birds. These ecosystems can be vegetation-dense, working to reduce water flow velocities through the wetland, acting to absorb wave energy during storm events, minimising the effects of storm surges on coastal areas and reducing the severity of erosion that can occur during these events (Spalding *et al.*, 2014; Department of the Environment and Energy, 2016). As climate change brings about increased storm severity, increased risk of erosion and rising sea levels, the importance of coastal wetlands is also likely to increase (Spalding *et al.*, 2014). The dense vegetation and reduced flow velocities encourage sedimentation and accretion of both organic and inorganic material within wetlands, working to increase the total elevation of associated coastal zones, which in some areas, may 'keep pace' with the 4 – 9 millimetre per year rate (lower threshold) of sea-level rise (SLR) predicted by the Intergovernmental Panel on Climate Change (IPCC) (Spalding *et al.*, 2014; Oppenheimer *et al.*, 2019).

3.1.1. Ecosystem Services

The benefits offered by wetlands, referred to as ecosystem services, are however, subject to variation with changing or degrading wetland ecosystems, and many coastal habitats are being lost at a rate that is up to four times faster than terrestrial forests (Spalding *et al.*, 2014). Threats arise from both direct and indirect sources. Direct sources include anthropogenic loss and fragmentation due to land claim, aquaculture, and mangrove harvest and overfishing, all of which can modify the ecosystem structure and function (Crooks *et al.*, 2011; Donato *et al.*, 2011; Spalding *et al.*, 2014). Indirect threats come from upland or upriver and include agricultural and other land-use-based run-off of excess nutrients, sediment or pollutants, which can also cause changes to the ecosystem function, both in the soil and in the water (Doroski, Helton and Vadas, 2019). Upstream damming and reduced water flows coupled with a changing climate can also put extra stress onto coastal wetlands (Spalding *et al.*,

2014). Urbanisation in coastal zones is another factor that threatens coastal wetlands. As sea-level rises, these habitats will naturally migrate landwards, but in places that infrastructure is built close to the coastal zone, this landward migration can only occur up until this anthropogenic barrier is reached (Donato *et al.*, 2011; Spalding *et al.*, 2014; Brown *et al.*, 2021). This threat is referred to as 'coastal squeeze' and can result in the drowning of coastal wetlands as they are unable to further respond to SLR.

The protective properties and ability to increase elevation with SLR leads to the opportunity for coastal wetlands to be used as an ''Ecosystem-based adaptation', or EbA, response to managing SLR across the globe and mitigating the hazards that coastal ecosystems and communities will face in a changing climate (Spalding *et al.*, 2014; Oppenheimer *et al.*, 2019). Implementing EbA strategies facilitates the restoration and conservation of coastal wetlands, not only providing the direct benefits in hazard mitigation, but also the wider benefits to the variety of life that depends on these ecosystems. However, the restoration and conservation of coastal wetlands can have even larger, and arguably more important and widespread effects. Specifically, this is their ability to sequester and store carbon in their sediments, more carbon than any other terrestrial ecosystem; globally the estimated sequestration rate is up to 87.2 ± 9.6 Tg Carbon per year (Donato *et al.*, 2011; Macreadie, Hughes and Kimbro, 2013). Figure 3.1 shows the magnitude of difference between different wetland systems themselves, and the overall difference between wetlands and other terrestrial environments.
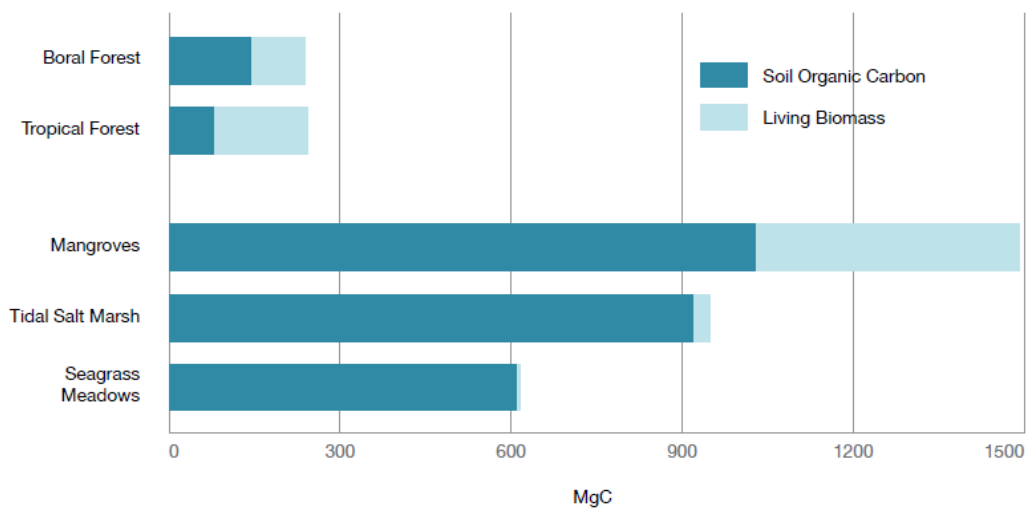
Figure 3.1: Mean above and below-ground sources of carbon in coastal wetlands compared with terrestrial forests (Howard et al., 2014). Carbon stock is measured per hectare.

3.1.2. Carbon Cycling and Greenhouse Gasses

Coastal wetland ecosystems receive large amounts of organic matter and nutrients from both ocean upwelling and land and river run-off, thus they can be highly productive ecosystems (Crooks *et al.*, 2011). Significant productivity supports the sequestration of large amounts of CO_2 from the atmosphere as both above ground biomass growth, and below ground as roots and rhizomes. As biomass dies and mixes with the soil profile, carbon is locked there by the constant tidal wetting of the soil, which inhibits rapid degradation back into CO_2, and subsequent burial by sediment supplied to the system (Crooks *et al.*, 2011). This cycle of biomass death, burial and trapping as soil carbon repeats, allowing the accretion of carbon-rich organic soils for millennia, rather than decadal or centennial timescales of terrestrial forests. Thus, carbon can accumulate for longer periods of time and build much larger stocks, as emphasised in Figure 1 (Crooks *et al.*, 2011). The rate of carbon burial for parts of the NSW Coast has been estimated to be 2.50 Mg C ha^{-1} year^{-1}; however, this value varies between vegetation assemblages (Saintilan et al., 2013). Gaseous emissions of CO_2 from saltmarsh have been found to be between $35 - 207$ mg C m^{-2} h^{-1}, as reported by Livesley and Andrusiak, (2012) for south-eastern Australia. Although, these values were obtained from the southern coast of Victoria, Australia, and due to the high variability of carbon budgeting arising from factors like rainfall regime, mean annual temperatures and vegetation structures, the reported flux values may be different to the NSW South Coast (Krauss *et al.*, 2018)

The process of carbon sequestration and storage may be interrupted as soon as any of the threats outlined in section 3.1.1 arise. Destruction of vegetative material may slow the system's ability to capture carbon, and any disturbance to the soil or to the tidal regime can switch the wetland from a carbon sink to a carbon source (Crooks *et al.*, 2011). Although, the removal of vegetation alone may not completely transition a wetland into a carbon source. Unvegetated mudflats also have the ability to fix atmospheric carbon, as they are inhabited by cyanobacteria and other microphytobenthos that drawn carbon from the atmosphere (Brown *et al.*, 2021). While the amount of carbon fixation is significantly less that from vegetated wetlands, mudflats can still bury up to 21 ± 6 g C m^2 year^{-1} (Brown *et al.*, 2021). However, carbon emissions as a result of land-use change and disturbance are not well understood, and is likely dependant on how deeply the soil is affected by disturbance (Donato *et al.*, 2011)

However, while not the focus of my research, it is important to note that CO_2 is not the only greenhouse gas (GHG) that is associated with coastal wetlands. Wetlands can also be a sink or source of both methane (CH_4) and nitrous oxide (N_2O) (Crooks *et al.*, 2011; Rosentreter *et al.*, 2021). Both gasses have higher global warming potential (GWP) than CO_2 (25 and 265 times that of CO_2, respectively) (IPCC, 2007).Hence, these gasses will still be included within this review of existing

literature, due to their importance as a GHG and the many ways that the environmental parameters looked at within this review affect them. The large GWPs of CH_4 and N_2O mean they have the potential to offset some, if not all, the sequestration and cooling effects obtained through wetlands trapping of CO_2 (Rosentreter *et al.*, 2021). Conversely, certain environmental conditions within wetlands could also increase the uptake of these higher-GWP gasses, enhancing the net cooling effects wetland may have. Understanding the conditions that lead to the formation of these GHGs in wetlands is an important aspect of understanding the long-term effectiveness of wetland ecosystem restoration in the context of global warming mitigation (Rosentreter *et al.*, 2021). How these GHGs are produced, and the conditions under which they occur will be detailed in the relevant sections within this review.

3.2. Environmental Variables

Interactions between environmental parameters like hydrology, salinity, soil characteristics and plant biomass can produce varied responses in GHG fluxes. Even within the same ecosystem, small changes in one parameter could lead to a source of GHGs, while another part acts as a sink (Krauss *et al.*, 2018). How fluxes respond to variations in these parameters will be described within the remainder of this section.

3.2.1. Tidal Inundation Duration and Extent

Inundation dynamics can be controlled through both tidal and non-tidal processes such as catchment inflows. The degree of control that either type of force has on a coastal water body leads to the formation of differing estuary types (Roy *et al.*, 2001). Estuaries with a more marine and tidal influence are classified as being either bays, or tide or wave-dominated estuaries. A stronger influence from non-tidal forces like freshwater catchment flows will result in entirely freshwater bodies, or estuaries that intermittently open to the open ocean (Roy *et al.*, 2001). Intermittently open and closed lakes or lagoons (ICOLLS), when open, are subjected to tidal inundation dynamics, which subject surrounding wetland vegetation – primarily saltmarsh – to cycles of inundation and exposure, and increased salinity (Hughes, Rogers and Wen, 2019). When closed, the ICOLL is subjected to elevated water levels, as catchment inflows, and rainfall are unable to escape. This creates a non-tidal environment, with varying salinity regimes due to the erratic and unpredictable rainfall patterns of south-eastern Australia (Roy *et al.*, 2001). The type of inundation regime that a coastal wetland is subject to in part controls how the wetland system will respond with respect to gaseous fluxes of GHGs.

Tidal inundation of coastal wetlands can trigger changes in the gas flux from the wetland's surface through biological pulses or by changing the composition of nutrients and substrates used by soil microbes (Emery *et al.*, 2021). Soil microbes consume organic matter contained within the soil profile, and through various biological respiration pathways, convert nutrients to energy and emit GHGs as an end-product of this process (Luo *et al.*, 2019). Emissions from wetlands have been found to be higher during the low periods in the tidal cycle, when more of the wetland's surface is exposed to air. Inundation events slow microbial respiration and subsequent gas emissions by interrupting soil-atmosphere gas exchange at the surface of the wetland, reducing microbes' ability to access the oxygen required for respiration (Emery *et al.*, 2021). A study published by Emery et al. (2021), which subjected wetland soil cores to simulated tidal, precipitative, and combined rewetting events, found that CO_2 emissions were halved by rewetting. The reduction in CO_2 emissions upon rewetting was immediate and lasted from 24 to 48 hours. However, the presence of some CO_2 emissions even under anoxic conditions indicates there is anaerobic respiration taking place (Emery *et al.*, 2021). A similar CO_2 reduction was experienced in a study monitoring a restored wetland, whereby upon restoration of tidal influence, CO_2 flux decreased by 95 g C m^{-2} year^{-1}.by (Negandhi *et al.*, 2019).

Emery *et al* (2021) also saw a sustained, rather than pulse-like, increase in CH_4 emission after rewetting. CH_4 formation, via methanogenesis, occurs from the microbial decomposition of organic matter within the soil profile, under strictly anaerobic conditions, as per the equation in Table 2.1 (Bange, 2006). Under more saline, anoxic conditions, however, sulfate reduction is typically the preferred pathway due to the sequential depletion of more energetically favourable electron
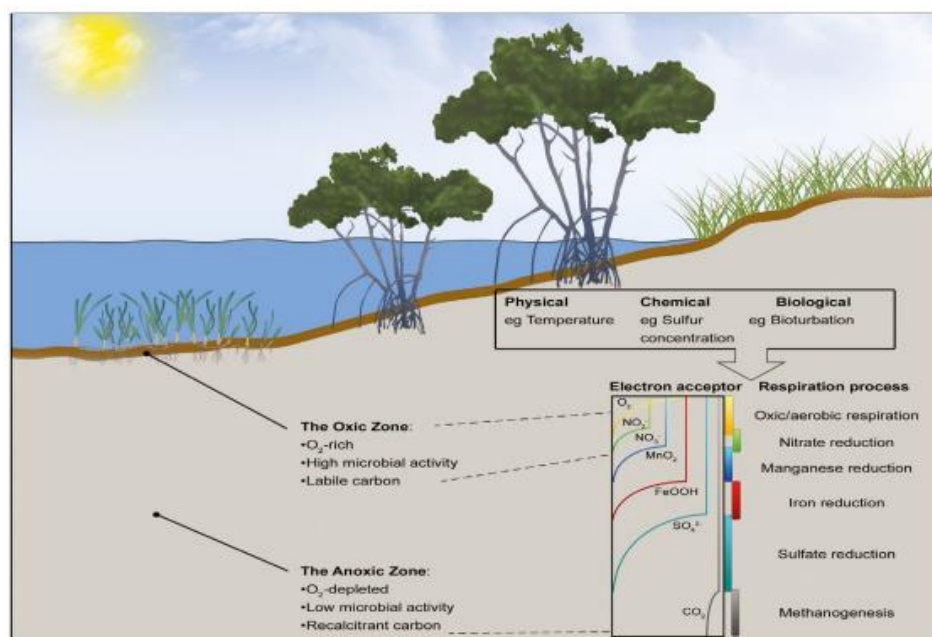
Figure 3.2:Factors that influence microbial respiration pathways within coastal wetlands. Also shown is the preferential use of electron acceptors, where sulfate reduction is preferable than methanogenesis. (Source from Macreadie et al., 2017).

acceptors before methanogens begin respiration (Luo *et al.*, 2019; Emery *et al.*, 2021). The order that electron acceptors are utilised, and their associated reaction pathways are shown in Figure 3.2 and Table 3.1. Electron acceptors are used in order of their relative energy yields (Table 3.1), and methanogenesis is the least favourable pathway, hence the presence of sulfates in the soil profile will trigger sulfate reduction as it is more energetically favourable (Chambers, Reddy and Osborne, 2011; Kristensen *et al.*, 2017; Luo *et al.*, 2019). The gradual increase in CH_4 seen by Emery *et al* (2021) was attributed to this gradual depletion of other electron acceptors brought into the system through simulated tidal inundation. However, the restoration of tidal flows monitored by Negandhi *et al.*, (2019) resulted in a net decrease in the CH_4 fluxes emitted from the wetland. This decrease was dwarfed by the effect of large rainfall events, which were removed to identify the net decrease in CH_4 fluxes post tidal flow restoration. The freshening effect of rainfall inundation further highlights the variability these coastal systems can exhibit, which may be further exacerbated by the unpredictable effects of climate change (Negandhi *et al.*, 2019).

The core experiment conducted by Emery *et al* (2021) showed a pulse of N_2O immediately after rewetting. N_2O can be produced through two pathways – nitrification and denitrification. During nitrification, N_2O is mostly a by-product, but under anoxic conditions, nitrifiers switch to the nitrifier denitrification pathway where N_2O becomes the primary end product (Bange, 2006; Emery *et al.*, 2021). Simultaneously, as oxygen is depleted, denitrifiers metabolise the nitrate produced by nitrification, creating a pulse of N_2O where they would normally produce N_2 under aerobic conditions. As the pool of nitrate is consumed, denitrifiers return to complete reduction to N_2, reducing the N_2O pulse (Emery *et al.*, 2021).

Table 3.1: Selected soil microbe respiration pathways and their associated reaction equations and standard free energy changes (Reproduced using equations from Lou et al., 2016)

Pathway	Reaction Equation	CH_2O (kJ mol^{-1})
Aerobic Respiration	$CH_2O + O_2 \rightarrow CO_2 + H_2O$	-475
Denitrification	$5CH_2O + 4NO_3^- \rightarrow 2N_2 + CO_2 + 4HCO_3^- + 3H_2O$	-448
Sulfate Reduction	$2CH_2O + SO_4^{2-} \rightarrow H_2S + 2HCO_3$	-77
Methanogenesis	$2CH_2O \rightarrow CH_4 + CO_2$	-58
Nitrification	$NH^3 + 1.5\ O_2 \dashrightarrow NO^{2-} + H+ + H_2O.$	

Inundation of coastal wetlands by tidal waters can decrease CO_2 emissions and increase emissions of N_2O, however, inundation can have mixed effects on the emission of CH_4. Gaseous emissions can be highly site-specific based of the inundation regime and can also be heavily influenced by large rainfall events, as demonstrated by Negandhi et al., (2019). As rainfall events, and similarly tidal inundation duration and extent are expected to increase with rising sea-levels and climate change, wetlands will be inundated for longer, and the inundation will be deeper, but also areas previously out of tidal reach will begin to experience flooding (Luo *et al.*, 2019). The potential increase emissions of the higher GWP gases may be offset by the sequestration ability of coastal wetlands and hence, monitoring of gas fluxes from coastal wetlands will be increasingly important to understand how they are currently responding, and will continue to respond to a changing climate and rising sea-levels (Crooks *et al.*, 2011; Oppenheimer *et al.*, 2019; Rosentreter *et al.*, 2021).

3.2.2. Soil and Water Salinity

Depending on the geomorphic setting within an estuary, salinity may be linked to tidal inundation duration and extent, as water is the vector for salt transport, and these salts will be brought into wherever the tidal water reaches. Salts will also deposit into the sediment layer that is wetted by the inundation event. Salinity exerts some control over carbon mineralisation and subsequent CO_2 emission rates through the stresses it puts on soil microbes who undergo respiration. According to a review published by Luo et al., (2019), most studies agree that increasing salinity has an inhibitory effect on carbon mineralisation rates. This is further backed by an experiment carried out on soil cores (Doroski, Helton and Vadas, 2019). Those results showed a suppressed CO_2 response across soil cores treated with both saltwater and sulfate-enriched water, when compared to a freshwater control. The suppression of CO_2 emission lasted throughout the experiment and did not return to pre-treatment levels. Hence, the potential for carbon mineralisation is likely lowest in brackish marshes; however, this could change depending on the hydrodynamic forces in an area – for example, a freshwater stream may discharge nearby, which would reduce saline stress and increase the potential for carbon mineralisation (Luo *et al.*, 2019). Trends in carbon burial rates have also been identified that show increased carbon burial with decreased salinity towards the upper estuary in tidal systems (Krauss *et al.*, 2018). Rates in forested freshwater tidal wetlands and freshwater marshes have been found to exceed those of low-salinity marshes and saltmarshes (90, 124, 93 and 40 g C m^2 $year^{-1}$, respectively) (Craft, 2012; Loomis and Craft, 2010).

Increases in salinity do not always have an inhibitory effect on carbon mineralisation. The findings present above apply to coastal wetlands, which are environments with an existing saline influence. When salinity increases in freshwater environments (less than 2.0 practical salinity units (psu) rates of carbon mineralisation can be increased, resulting in increased carbon emissions (Krauss *et al.*, 2018). Where the baseline inundation regime of these freshwater systems is typically water >2 psu, the primary respiration pathway is via methanogenesis; however, exposure to saline water can switch the respiration pathway to sulfate reduction, and if sustained, can double the rate of carbon mineralisation (Krauss *et al.*, 2018; Rogers *et al.*, 2019). Even a short pulse of saline water into freshwater habitats is enough to sustain carbon losses for multiple months after exposure has occurred. (Krauss *et al.*, 2018). Over time, continuing saline pulses have the potential to shift freshwater systems towards increased rates of carbon mineralisation via sulfate reduction pathways (Krauss *et al.*, 2018). Such an occurrence would lead to heightened CO_2 emissions as SLR occurs and freshwater ecosystems are more frequently exposed to saline tidal waters. This would create a positive feedback loop, further exacerbating global warming. As a result of salinisation, there is a strong, negative correlation between salinity and CH_4 fluxes, due to increased presence of more energetically favourable electron acceptors facilitating sulfate reduction over other pathways (Luo *et al.*, 2019). This is consistent with findings presented by Moseman-Valtierra *et al.*, (2016), in which high CH_4 emission events corresponded with low salinities. The contrasting influences that increasing salinity may have on wetland environments on carbon fluxes – both CO_2 and CH_4 – means that further research is necessary to understand how they will respond to SLR and salinisation, and what climate feedbacks may occur.

3.2.3. Soil Characteristics and Soil Carbon Content

The geomorphic setting that a wetland is contained within can have an overarching control over the biological, physical and biogeochemical processes that are responsible for carbon accumulation and storage (Roy et al., 2001; Kelleway et al., 2016a). As a consequence of this, there can be substantial variation in carbon stores between wetlands locally and globally (Kelleway et al., 2016a). The role of vegetation in carbon fixation via photosynthesis is discussed in section 3.2.4, but the geomorphic setting controls factors that trap the carbon and store it within the soil profile, and one of these key factors is soil characteristics (Kelleway et al., 2016a). Two broad geomorphic settings can be identified in estuaries; those with a more marine influence have moderately well-sorted sands with lesser amounts of mud, and those with a more dominant fluvial, or mixed influence, have ranging sediment compositions of poorly sorted mixtures of sand, mud and organics to mud and organic-rich sediments (Kelleway et al., 2016a). A growing link has been found that there is a relationship between depositional settings and the carbon stored within the soil. Marsh habitats located near to fluvial

influences have a greater carbon store than those with a more marine influence (Kelleway et al., 2016a; Macreadie et al., 2017; Gorham et al., 2021). In Western Australia, fluvially-influenced marshes had up to 1.3 times more carbon than marine-influenced marshes (Gorham *et al.*, 2021). While coastal wetland systems along the NSW Coastline on average, have more than double the store of carbon in fluvially-influence settings than in those with a marine influence (226.09 ± 12.37 Mg C ha^{-1} and 104.54 ± 7.11 Mg C ha^{-1} respectively. A further breakdown of these values is provided in Table 3.2 (Kelleway et al., 2016a). Sediment grain size was found to be the primary explanatory variable for carbon density in Southern NSW estuaries, with finer-grained sediments having significantly higher carbon densities than mixed and sandy sediments, in that order (Kelleway et al., 2016a).

Table 3.2: Organic carbon stocks found in different vegetation stands in fluvial and tide-influenced saltmarsh settings. Values are averages and are presented with standard errors. Values are Megagrams of carbon per hectare. (Reproduced via Kelleway et al. 2016).

Vegetation Community	Fluvial Influence Carbon Density (Mg C ha^{-1})		Marine Influence Carbon Density (Mg C ha^{-1})	
	Mean	**SE**	**Mean**	**SE**
Rush	215.8	25.7	118	25.8
Succulent/grass	232.9	25.5	91.8	25.5
Saltmarsh (whole)	164			

One mechanism that may be a factor for finer sediments having higher carbon densities is sediment porosity. Bulk density is a function of grain size, and soils with lower bulk densities have more pore space between soil aggregates (Ball, 2013; Morris *et al.*, 2016). Sandy soils have more rapid drainage from a larger porosity, which allows for exposure of soil carbon to the atmosphere, likely causing more rapid mineralisation and emission of carbon from the soil (Kelleway et al., 2016a). Finer-grained sediments would however show opposite characteristics, having a smaller porosity, holding onto water for longer and hence not exposing trapped carbon to the atmosphere, lessening carbon emissions. However, a contrasting pattern was found during a review, where pore spaces tended to be larger and bulk density lower in freshwater to brackish sediments, which would allow for more contact between organic matter and the atmosphere and promote aerobic respiration and CO_2 emissions (Hedges and Keil, 1995; Luo *et al.*, 2019; Gorham *et al.*, 2021).

Soil moisture is typically recorded as the percentage of measured soil that contains water, calculated after drying. The moisture content is controlled by both the tidal inundation and precipitation regimes, but also by the soil characteristics as discussed above. As outlined in Sections 3.2.1 and 3.2.2, a higher moisture content can create increasingly anoxic conditions, decreasing CO_2

emission and increasing CH_4 production, or under more saline conditions, will cause the production of SO_2. However, there may be an optimal moisture content for microbial respiration. Wickland and Neff, (2008) suggested that respiration peaked when the moisture content of the soil was approximately 75 percent, however local variation in soil characteristics and microorganism communities could lead to the optimal moisture content varying spatially (Yin *et al.*, 2019).

3.2.4. Biomass/vegetation variation

The plant species in an area, and their subsequent productivity and biomass will ultimately depend on the environmental conditions in that area. In the context of this thesis, plant distribution and biomass will be discussed within the environmental parameters outlined in sections 3.2.1 through 3.2.3. Both inundation and salinity are stressors on plants, and can negatively impact their productivity, biomass, and carbon sequestration capacity (Lill *et al.*, 2013; Moseman-Valtierra *et al.*, 2016; Luo *et al.*, 2019). Though, in brackish wetlands, salinity may allow for higher biomass as the selective pressure of more saline waters increases competition and increases the presence of nutrients like ammonia (NH_4^+) (Luo *et al.*, 2019). Inundation can be seen as a driver of vegetation variation through its partial control over salinity, directly by tidal inundation, but also if inundation is not occurring (for example, in a closed ICOLL) then saltmarshes can become increasingly saline as water is evaporated (Saintilan, 2009). This will then determine where the salt-tolerant species exist (Saintilan, 2009; Luo *et al.*, 2019). Inundation acting in this way naturally leads to more salt-tolerant species out-competing non-tolerant species as sea-levels rise. Variation in vegetation distribution can also be a factor of tidal inundation itself, as tidal currents may dislodge seedlings and transport propagules, or turbid waters may deposit sediment on leaves of plants, lowering their photosynthetic capacity (Saintilan, 2009).

3.2.4.1. Community Variation on NSW South Coast

The variation and distribution of vegetation types within the location of interest, being the NSW South Coast, typically shows a zonal distribution of vegetation along a gradient, beginning at approximate mean sea-level, through to the supratidal zone, above the Highest Astronomical Tide (Saintilan *et al.*, 2019). The tidal inundation regime creating this gradient are also affected by changes in elevation on both macro and micro-scales. Mangroves are normally constrained to below mean high water and above mean sea-level. *Avicennia marina* is the abundant mangrove species in this region but may be absent from ICOLLS (Kelleway *et al.*, 2017). Stands of *Casuarina glauca* or *Melaleuca ericifolia* typically inhabit areas above mean high water, where there is little tidal inundation (Saintilan *et al.*, 2019). Between these two communities lies the saltmarsh, where different vegetation types are likely to occur in either upper or lower sections, each generally having a low species richness of one

or two dominating plant species, particularly towards the lower elevations that are more frequently inundated (Saintilan, 2009; Kelleway et al., 2016a; Mills, 2021).

The species richness can increase further up the saltmarsh zones but can again be reduced if there is a freshwater input facilitating the growth of tall competitive and dominant species like *Phragmites* and *Typha* (Saintilan, 2009). Low to mid marsh zones are typically inhabited by *Sarcocornia quinqueflora*, a low-growing succulent, and *Sporobolus virginicus*, a grass, while the upper zone of the marsh is dominated by *Juncus kraussii* and *Baumea juncea*, however, a mosaic of vegetation types may also occur (Kelleway et al., 2016a). Biomass is typically higher in the rush-dominated communities (*Juncus* = 1116 g m^2) versus the non-rush communities (320 and 350 g m^2 for *Sarcocornia* and *Sporobolus,* respectively) (Kelleway *et al.*, 2017). Some saltmarshes also have algae communities that form where there is little-to-no coverage of vegetation, or on hyper-saline tidal flats (Saintilan, 2009; Kelleway *et al.*, 2017). However, the occurrence of hyper-saline patches within NSW marshes is small, compared to tropical counterparts (Saintilan, 2009).

3.2.4.2. Plant driven GHG Variations

Variations in GHG emissions are influenced by the distribution and presence of vascular plants, the species composition and abiotic and biotic factors (Moseman-Valtierra *et al.*, 2016). Some marsh plants that occupy the lower marsh, which is more prone to inundation, contain features such as aerenchyma, which are gas-filled spaces within the plant tissue that facilitate gas exchange and keep roots oxygenated during anoxic conditions. It is these aerenchyma that may increase fluxes of GHGs from anoxic soil conditions, despite the soil-atmosphere gas exchange being interrupted by overlying water (Moseman-Valtierra *et al.*, 2016). High-marsh zones can be inhabited by species that are denser, with shallow roots, adaptations that result in less ventilation of soils and lower GHG fluxes. In coastal marsh areas in New England, USA, CO_2 fluxes were highly correlated with belowground biomass, and moderately with aboveground biomass, which may reflect that lower-marsh plants have larger gas fluxes than higher marsh plants with shallower belowground biomass (Moseman-Valtierra et al., (2016).

Emissions of GHGs also vary on a temporal scale. Typically, as plants are photosynthesising throughout the day, net fluxes of CO_2 tend to be smaller, or more negative as plants draw in CO_2. At night, photosynthesis pauses, and respiration is the dominant process occurring, hence fluxes of CO_2 tend to be more positive as CO_2 is released (Moseman-Valtierra *et al.*, 2016; Abdul-Aziz *et al.*, 2018) Both sunlight and soil temperature have been found to have moderate to strong control over daytime CO_2 uptake by plants in North American saltmarshes, as increased temperatures accelerate the rates of photosynthesis in some plants. However, photosynthetic rates can be reduced should temperatures

climb too high (Abdul-Aziz *et al.*, 2018). This may have complex implications for saltmarsh and their capacity to both survive and sequester carbon from the atmosphere under increasing global warming. While CO_2 fluxes did vary temporally, there was no difference in CH_4 fluxes between day and night-time, as CH_4 fluxes are not directly driven by sunlight or photosynthesis (Moseman-Valtierra *et al.*, 2016). Vegetative growing cycles throughout the year also lend to seasonal variations in the GHGs fluxes from plant communities. CO_2 fluxes can be expected to be more negative during the growing seasons of plants – typically spring through early summer (Emery and Fulweiler, 2014).

3.2.4.3. Vegetation Controls on Soil Carbon Variation

Variation in plant species and community composition creates differences in the soil carbon content throughout a coastal wetland system. Differences in the structural properties and productivity between species can influence the capacity of a vegetation community to directly contribute to the carbon pool through growth, but also by capturing and retaining sediment and organic material from surrounding communities (Kelleway et al., 2016a). The roots and rhizomes of a plant are also a significant source of organic matter into the soil, so plants with a larger biomass, more roots and a high rate of turnover are likely to contribute more carbon to the soil (Kelleway *et al.*, 2017). Rates of carbon sequestration can vary between vegetation types and communities, as found by Lovelock et al., (2014) in Southeast Queensland. Here, *J. kraussii*-dominated marshes had a higher rate of carbon sequestration than marshes dominated by *S. quinqueflora*. Variation in carbon accumulation rates was also studied by Saintilan et al., (2013), who found that rates of accumulation depended more on the hydro-geomorphic setting rather than the vegetation type.

Despite rates of carbon sequestration potentially varying both within and between coastal saltmarshes, stocks of carbon in the soils of saltmarsh does not vary by vegetation, but by geomorphic setting, as outlined in section 3.2.3 (Kelleway et al., 2016a). The drivers of the difference between marine and fluvially influenced marshes are complex, but outside the realm of my research, however, the difference remains important, nonetheless. If carbon stocks are higher within fluvial marsh systems that are hydrodynamically connected to tidal deltas and marsh areas, then they stand at risk of salinisation and subsequent carbon mineralisation from rising sea-levels.

Surface sediment accretion is important to maintain as it ensures the survival of the saltmarsh under SLR (Kelleway *et al.*, 2017). Inputs of sediment can be derived from within the saltmarsh, or come from adjacent environments, and accreted sediment and organic matter eventually will become part of the soil carbon pool in a site. *J. kraussii*-dominated marsh zones, given their higher biomass and stable input of organic matter to the soil, combined with less tidally driven export of decaying material, allows for higher rates of accretion (Kelleway et al., 2017; Saintilan et al., 2013).

Contrastingly, marsh dominated by *S. quinqueflora* and *S. virginicus* is subject to more regular tidal flows, which act to 'clean' the surface and export decaying organic material, lowering the rate of accretion (Saintilan *et al.*, 2013).

The GHG flux response arising from the vegetation-controlled variations in soil carbon is less well researched. The response of coastal wetlands to SLR may be mixed, as salinisation of freshwater zones may cause increased carbon mineralisation, yet mangrove encroachment forced by rising sea-levels has been found to increase carbon stores beneath new mangrove habitat (Kelleway et al., 2016b). How these gas fluxes vary is a key component of this research report and data collection from the Tilba Lake study site.

3.3. Soil Carbon and Net Ecosystem Exchange

The transfer of carbon, between the biosphere and the atmosphere is referred to as the Net Ecosystem Exchange (NEE) (Restaino and Peterson, 2013). NEE is measured as carbon per unit of ground area per unit time and is an indicator of the strength of an ecosystem to act as either a sink or source (Restaino and Peterson, 2013). Some examples of NEEs from around the globe are presented in Table 3.3.

Table 3.3: Examples of NEEs from different environments around the world. Negative values indicate an exchange towards the ground, or uptake of carbon by an ecosystem. A positive value indicates a net release of carbon to the atmosphere

Location	Net Ecosystem Exchange	Source
Morgan Monroe State Forest (USA)	236 g C m^2 year^{-1}	(Reichle, 2020)
Managed grassland (Ireland)	-189 g C m^2 year^{-1}	(Dondini *et al.*, 2018)
Himalayan Pine Forest (India)	-99 g C m^2 year^{-1}	(Singh *et al.*, 2019)
Dry tropical forest (Brazil)	-169 g C m^2 year^{-1} (2014) -145 g C m^2 year^{-1} (2015)	(Mendes *et al.*, 2020)
Salt Marsh (Massachusetts, USA)	-179 g C m^2 year^{-1}	(Forbrich, Giblin and Hopkinson, 2018)
Managed Urban Tidal Marsh (New Jersey, USA)	-65 – 310 g C m^2 year^{-1}	(Krauss *et al.*, 2018)
Tidal Freshwater Marsh (Louisiana, USA)	290 g C m^2 year^{-1}	(Krauss *et al.*, 2018)
Restored Tidal Wetland (California, USA)	397 – 804 g C m^2 year^{-1}	(Krauss *et al.*, 2018)

A means of measuring NEE is the eddy Covariance (EC) method, which will be introduced in more detail in the following section. The use of EC to measure NEE is beneficial as it can be utilised over multiple timeframes (Reichle, 2020). However, NEE itself does not factor carbon losses from other sources, such as lateral loss of dissolved carbon or losses associated with disturbance, or loss as Volatile Organic Compounds (VOCs) (Reichle, 2020).

NEE is calculated as the difference between the Gross Ecosystem Production (GEP) and the Ecosystem Respiration (R_{eco}), that is:

$$NEE = R_{eco} - GEP$$

GEP represents the total amount of carbon taken up by an ecosystem, while R_{eco} is the carbon released by plants during respiration (Reichstein *et al.*, 2005). The splitting of the overall flux into its respective parts can help to understand interannual and seasonal variations when EC data exists across a wide temporal scale. For instance, when splitting the NEE into its two parts, R_{eco} would be expected to be much higher during the plants growing season when it is respiring more than during periods of dormancy (Reichstein *et al.*, 2005). The seasonal variations in NEE are related to changes in abiotic variables throughout the year, factors such as photosynthetically active radiation, air and soil temperature and precipitation (Peichl *et al.*, 2014). The level of the water table may also have an influence over NEE seasonally, as its position controls both plant productivity and the rate at which decomposition can occur(Peichl *et al.*, 2014). The variability of NEE as a result of changes in abiotic factors also highlights the susceptibility of these system to climate change, as a warmer and drier climate may increase decomposition and subsequent carbon emissions (Peichl *et al.*, 2014). This shows the importance of understanding how environmental variables can affect GHG fluxes within wetland environments to predict the future impacts of climate change.

3.4. The Eddy Covariance Method

Fluxes, as mentioned earlier, in the context of this research refers to the amount of gas - CO_2 and H_2O – passing through a plane of unit area per time unit. This plane can exist both parallel to and perpendicular to the ground. Only a ground-parallel plane is of interest in this study, as vertical fluxes from the wetland surface are of interest. A flux is dependent on the size of the area that the gas is passing through, the amount of gas, the time taken, but also the ambient weather conditions exerting control on the air parcel's motion (Burba and Anderson, 2010). A negative flux indicates an overall net downward motion of gas, likely due to plants absorbing CO_2 for photosynthesis during the day, while a positive flux indicates a net upwards motion – emission – of gas from the grounds surface (Burba and Anderson, 2010). Of the common methods chosen for measuring fluxes in coastal wetlands, the eddy co-variance method was selected for my study site. The eddy co-variance towers (EC towers) measure the net flux in and out of a 'box' of space. For example, if ten molecules of CO_2 left the 'box' upwards, then only five returned back down, then the net flux was upwards – a positive flux of CO_2 leaving the 'box'. This net exchange of CO_2 in and out of the box in subsequent eddies are contained within a much larger, overall air flow motion, which contains many eddies within it (Burba and Anderson, 2010). The instrument mounted on the EC tower rapidly samples many of these eddies as they pass through, allowing an overall flux to be given. The instrument is also able to monitor wind speed and direction on all three axes (one vertical and two horizontal). The speed and direction of the flux allows a footprint to be determined – that is the area from which that parcel of air and its contained gases originated. There are a number of assumptions however, that go into the automatic calculations carried out in the instruments processing of the data. It is assumed that there is an adequate fetch, that is the terrain in the upwind distance is uniform, to ensure that the measured flux only comes from the area of interest and is representative of that area, and not contaminated by fluxes from distant sources (Burba and Anderson, 2010; Drexler et al., 2004). Other assumptions are that the measurements are done within the boundary layer of interest, and that density fluctuations and flow divergences and convergences are negligible (Burba and Anderson, 2010).

The boundary layer is the atmospheric layer of interest, and is typically 20-50 metres high, when the atmosphere is unstable and consequentially unstratified (Aubinet, Vesala and Papale, 2012). The thickness of this layer can reduce if the atmosphere becomes more stable and stratifies. Stability is the resistance of the atmosphere to vertical motion, and it can change throughout the day, as it is controlled by the energy available – more energy will reduce stability as there is more turbulence and more mixing in the atmosphere, and this typically occurs during the day. These conditions are optimal for the instruments used in the EC method, as it ensures adequate mixing of gases to obtain a representative sample (Drexler *et al.*, 2004). At night, when there is less energy entering the

atmosphere as heat, stability increases, and stratification can occur. During stratification, layers of the atmosphere do not mix, which can lead to the same air parcel remaining around the detection instruments on the EC tower, which is not ideal for obtaining representative samples.

3.4.1. Alternative Flux Measurement Methods

In addition to the EC Method outlined in section 2.4, there are two additional ways of measuring fluxes in salt marsh environments; henceforth the Chamber Method, and the Soil Core Method.

The Chamber Method involves setting up a space that can capture gases – a chamber – over the top of an ecosystem. This chamber can be opened and closed as necessary to conduct measurements. A field-based study that utilised the Chamber Method was carried out by Chojnicki, Acosta and Augustin, (2014) in a freshwater wetland in Poland. While the environment was not a salt marsh, the general approach of using chambers can be used in coastal ecosystems. Their chambers were constructed out of PVC, in a quadratic prism with a total volume of 0.3 cubic metres. Within the chamber, an infrared gas analyser, thermometer and soil temperature probes were installed to collect data, while a second thermometer was mounted outside for comparison of internal and external temperatures. The way in which the chambers were set up by Chojnicki, Acosta and Augustin, (2014), allowed for near constant measurement of fluxes, but only allows a small spatial scale to be sampled, unless multiple chambers are established over an area, which can be expensive. Different plant communities within a wetland can be sampled independently of one another using chambers but does not allow for larger spatial scale samples as eddy Covariance does. Sampling of vegetation can also be disruptive, as the chamber needs to be placed over the vegetation, in a way that it can meet the ground.

The alternative, the soil Core Method, is more lab-based than either the Chamber or EC Methods. It involves taking soil cores from the ecosystem of interest and taking them to a lab where the cores are subjected to a range of experimental treatments. For example, Emery et al., (2021) subjected saltmarsh soil cores to treatments simulating tidal, storm, and combined storm and tidal inundation events to measure the effect of these events on GHG fluxes. A different soil core experiment, conducted by Doroski, Helton and Vadas, (2019) subjected tidal wetland soil cores to treatments of fresh and seawater, elevated sulfate, elevated nitrate and copper, and combined nitrate and copper. This simulated the effects of saltwater intrusion, urban pollution run-off, and a combined effect of the two on GHG fluxes. The Soil Core Method allows for more controlled experimental treatment than EC, which only allows for capturing of the natural variability, which is obviously the strength of EC. Soil core experiments may also be cheaper to carry out, as the instruments required for EC are expensive, and when field-based, are subject to weather and tidal conditions that place them at risk.

3.5. Blue Carbon Sampling and Estimation

Blue carbon includes carbon that is stored within four main smaller pools in the coastal environment. These pools include above and belowground living biomass (branches, leaves, roots and pneumatophores), non-living biomass (dead wood and leaf litter) and the carbon held within the soil itself (Howard *et al.*, 2014). Blue carbon can be categorised two ways; autochthonous carbon is grown, deposited, and buried within the same area, while allochthonous carbon is brought into an area from another through hydrodynamic vectors (Howard *et al.*, 2014). To understand further how blue carbon systems can help mitigate global warming, and to address this role of blue carbon through policy and other regulatory frameworks, it is important to be able to quantify the stocks of blue carbon that exist within coastal ecosystems (Howard *et al.*, 2014). Accounting of carbon stocks can be done at site-specific, regional, national or global scales to create inventories, and this can be done to one of three tiers of accuracy to align with methods described by the IPCC.

Table 3.4: Mean values carbon stocks in the top metres of soil for the three primary coastal wetland environments both globally and within Australian coastal ecosystems (Reproduced from Howard et al., (2014) and Serrano et al., (2019) respectively). N/R = not reported.

Coastal Ecosystem	Carbon Stock (Mg ha^{-1})	± One Standard Deviation
Mangrove (Globally)	386	N/R
Saltmarsh (Globally)	255	N/R
Seagrass (Globally)	108	N/R
Mangrove (Australia)	251	155
Saltmarsh (Australia)	168	127
Seagrass (Australia)	112	88

3.5.1. Estimating Blue Carbon Stocks

At tier one, the lowest level of accuracy, when no site-specific data exists, carbon stocks are calculated using the global mean carbon stock for the primary vegetative ecosystem, as displayed in Table 3.4 and multiplying it by the size of the given area (Howard *et al.*, 2014).

The belowground biomass pool of coastal saltmarsh contributes a large proportion of the overall carbon stored within an ecosystem (Howard *et al.*, 2014). It can also be hard to separate from the non-living soil carbon pool, hence they can be treated as a single pool without compromising the accuracy of the inventory assessment (Howard *et al.*, 2014). This combined pool is an important stock of carbon, as the soil component can account for upwards of 98 percent of the total carbon in tidal saltmarshes (Howard *et al.*, 2014).

To begin estimating carbon stocks to a level of detail greater than tier 1 as described by the IPCC, Howard et al., (2014) outline a sampling and analysis method. Necessary parameters of soil depth, dry bulk density (DBD) and soil organic carbon content ($\%C_{org}$) must be determined for an estimation to be carried out. Determination of necessary parameters generally involves taking soil cores from an adequate spread of a coastal wetland, and sampling down the depth profile of each for DBD and $\%C_{org}$. Cores should be taken to a minimum depth of one metre but are commonly sampled to between three and five metres. There are several methods of determining $\%C_{org}$; elemental analysers give a quantitative measure of carbon within a sample, but instruments can be expensive to purchase and maintain. A wet combustion method uses chemical digestion reactions but can involve incomplete reactions and produces toxic waste. A method that is both cheaper and more reliable than the previous option respectively, is loss on ignition (LOI). LOI burns off organic matter from soil samples, and the resulting weight difference is used to determine the organic matter component, from which the $\%C_{org}$ can be empirically derived (Howard *et al.*, 2014). Empirical equations are provided by Howard et al, however these are specific to regions outside of Australia (table 3.5).

Table 3.5:*Empirical equations relating the organic matter content established through LOI to the organic carbon component within the soil.*

Ecosystem	Relationship Strength (r^2)	Empirical Equation	Location (Source)
Tidal Salt Marsh	0.98	$\%C_{org} = 0.47 * \%LOI + 0.0008 * (\%LOI)^2$	Maine, USA (Howard *et al.*, 2014)
Tidal Salt Marsh	0.99	$\%C_{org} = 0.4 * \%LOI + 0.0025 * (\%LOI)^2$	North Carolina, USA (Craft, Seneca and Broome, 1991)

The LOI method may result in overestimation of $\%C_{org}$ if the soil is overly clayey – due to the loss of structural water – or if the soil contains larger proportions of carbonate material – inorganic carbon can be lost at combustion greater than 500°C (Howard *et al.*, 2014). Despite these limitations, the LOI method has been demonstrated to be a reliable method to determine $\%C_{org}$ (Craft, Seneca and Broome, 1991)

Once the above parameters are determined, the total soil in each core can be estimated and converted to a value of carbon per unit area. Cores can then be averaged over any sampling strata that are present in the area, resulting in an estimation of the total soil carbon inventory in a coastal wetland.

3.5.2. Sampling Vegetative Carbon Pools

A complete picture of the carbon stored within an ecosystem cannot be formed without also estimating the carbon stored within above-ground biomass. For best estimates, samples should be taken when biomass is at its greatest (Howard *et al.*, 2014). Sampling across seasons also grants more insight into how biomass and carbon stores vary throughout the year, but samples must be collected at the same time each season (Howard *et al.*, 2014). Howard et al., (2014) suggests measuring stem number and height of rush-like vegetation (i.e., *J. Kraussii*) to develop allometric equations to determine for biomass. A biomass amount can then be multiplied by a species-specific carbon conversion factor to determine the amount of carbon stored within vegetation. However, this method may not be practical for all saltmarsh species that show weak relationships between height and biomass (Owers, Rogers and Woodroffe, 2018). Hence, the use of allometric equations may yield inaccurate estimations of biomass and carbon stores within a salt marsh environment. An alternative approach, albeit still destructive, is to establish replicate plots within and across vegetation strata and harvest all standing plant material within each plot (Clarke and Jacoby, 1994). Vegetation should then be dried to constant mass, and the biomass component can be multiplied by a carbon conversion factor (a factor of 0.45 is suggested by Howard et al., (2014) for grasses, sedges and other herbaceous plants). This can then be scaled up to the appropriate scale of different vegetation types, and the saltmarsh as a whole, if needed.

4. Site Selection and Characterisation:

The saltmarsh studied as a part of this research project is located on the edge of Tilba Tilba Lake (Tilba Lake), on the New South Wales South Coast (36°18'33'' S 150°07'11'' E) (Figure 4.1) Tilba Lake is an ICOLL, an Intermittently Closed and Open Lake or Lagoon, the mouth of which, when open, drains into the ocean. When open, the estuary is subject to tidal cycles. The wider area of the wetland is approximately 6.9 hectares in area, as indicated in yellow in Figure 4.1. The wetland consists of a main saltmarsh which is fronted by a small tidal channel that is approximately five metres wide when the marsh surface is exposed during an open ICOLL phase.

Tilba Lake and the Extent of the Monitored Saltmarsh

Service Layer Credits: Source: Esri, Maxar, GeoEye, Earthstar Geographics, CNES/Airbus DS, USDA, USGS, AeroGRID, IGN, and the GIS User Community
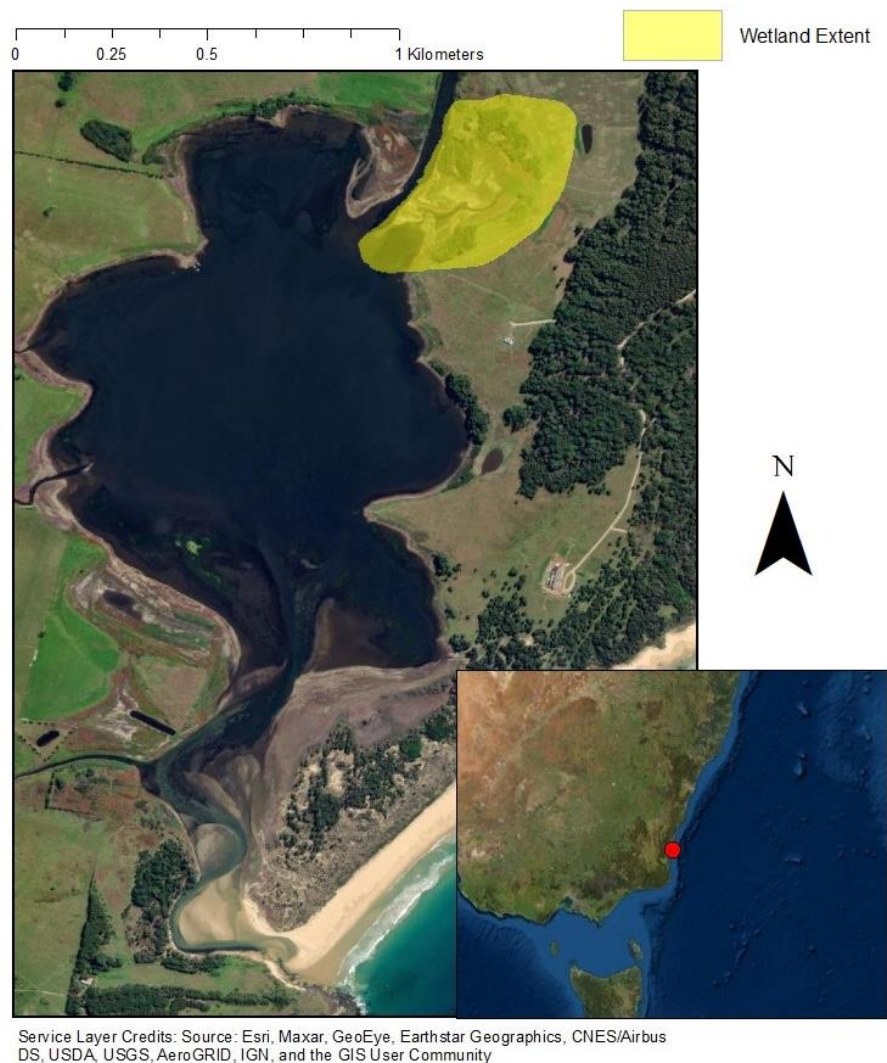
Figure 4.1: Map showing the location of Tilba Tilba Lake, and the extent of the saltmarsh monitored as a part of this research project

The site was selected due to a number of factors. Local Land Services (in conjunction with the NSW Government Department of Planning, Industry and Environment (DPIE)) have been undertaking management actions in the Tilba Lake Catchment to improve water quality in the lake. Landowners around the lake can participate in the program, and the owner of the land that the saltmarsh sits on allowed a long-term research program to occur to monitor GHG fluxes, which this project sits within. The site was previously grazed by livestock, which are now excluded from the area as part of the ongoing management program. The private property is also beneficial as it allows a secure site to establish expensive, long-term monitoring instruments without the threat of theft or interference. The smaller size of the wetland also allows for a more constrained vegetation footprint for utilisation of the eddy co-variance method - outlined in section 3.4 - to measure gas fluxes.

The vegetation zonation of the marsh shows a marked change from the tidal channel towards the high end of the marsh. The channel is flanked by small patches of mudflat on both sides. On the northern side of the channel, the marsh transitions through multiple vegetation communities, which are displayed in Figure 4.2 Henceforth, the vegetation communities will be referred to in the following manner.

- 'Sarcocornia' Community: This community consists almost completely of *Sarcocornia quinqueflora*. At the interface of this and the Juncus community, the two dominant vegetation types intermix with one another, forming a patchy mosaic.
- 'Juncus' Community: This community is dominated by stands of *Juncus krauss ii*, intermixed with *S. quinqueflora, Paspaylum distichum, Samolus repans,* and *Trigloghin striatum*. The Juncus community borders both the Phragmites and Melaleuca communities, forming a more abrupt transition into both than the Sarcocornia community.
- 'Phragmites' Community: This community is dominated by *Phragmites australis*, but still contains all of the same species as the Juncus community, however with significantly less *J. kraussii*.
- 'Melaleuca' Community: This community contains less species diversity, instead consisting mostly of mature *Melaleuca ericifolia* trees. This community is located at the end of the transect, at the highest point at the northern end of the marsh.

The marsh surface contains some depressions that form pools following rainfall or some high tides. There is also evidence of dried algal mats that have been captured by taller vegetation, primarily *J. kraussii*.

A transect was established to capture changes in the vegetation through the Sarcocornia, Juncus and Melaleuca communities, ending at a groundwater standpipe in the latter community. The transect begins at the point in the middle of the tidal channel that fronts the marsh – this point is where the tidal channel water logger is placed. The transect then runs perpendicular to the tidal channel for 210 metres, and has an elevation increase of approximately 1.14 metres from beginning to end. Points were marked along the transect using PVC pipes, and these locations were used as soil sample reference points and locations of the groundwater standpipes (sections 5.2.1 and 5.1.1 respectively). The Phragmites community was not directly on the sample transect; it was located approximately 30 metres to the east. Samples were still collected in the Phragmites community to assess how environmental variables may change with the vegetation. This community was not subject to GHG measurements.
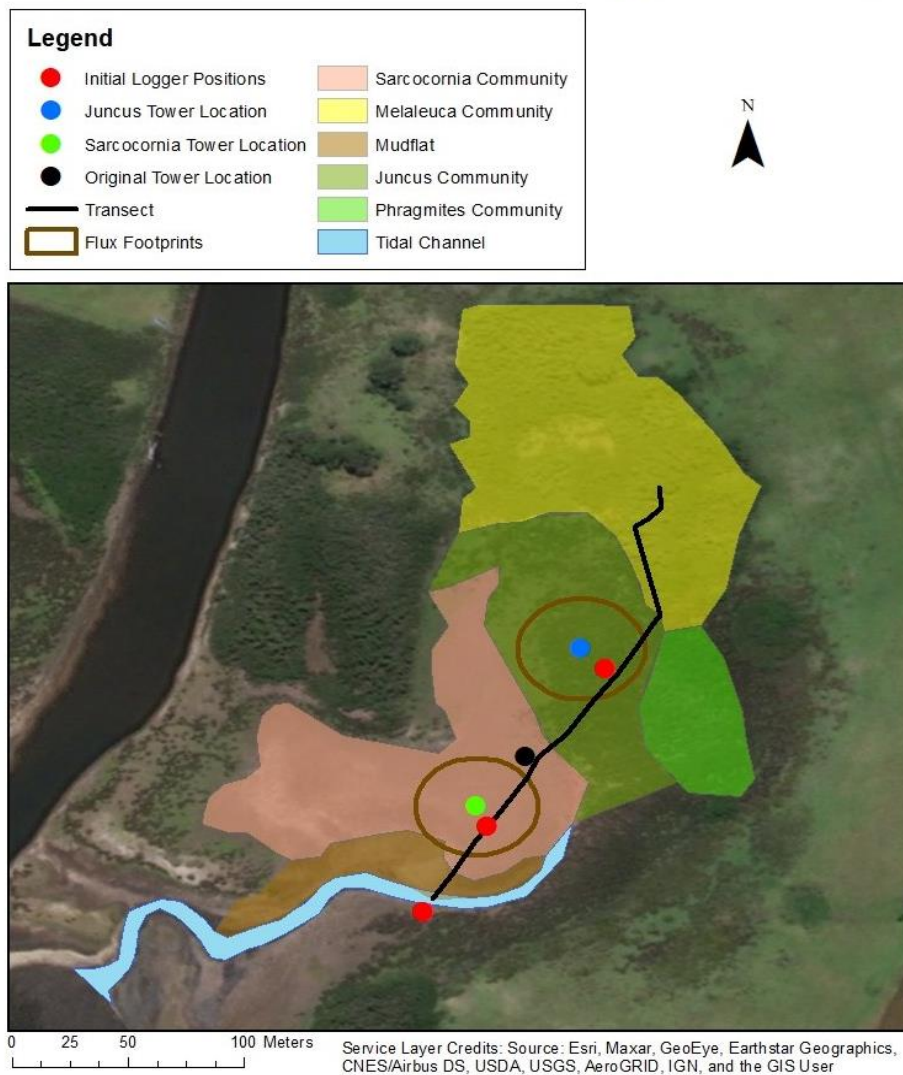
Figure 4.2: Map showing the different vegetation communities throughout the Lake Tilba saltmarsh. Also included are the locations of both current eddy co-variance towers, the location of the initial tower, the location of the initial three water loggers and the path of the transect.

5. Methods:

5.1. Sensor Equipment Placement

5.1.1. Water Level and Salinity Loggers

Automated loggers were deployed at multiple locations across the study site (Figure 4.2). These located enabled capturing of temporal and spatial variation in water level and salinity of ground and surface water. Three Loggers had already been deployed to the Tilba Lake study site before the commencement of this research project, as part of the larger, still on-going project. One of these loggers (HOBO U20L) collects only water-level data, and was placed in the centre of the channel surface, as in Figure 4.2. The remaining two water level and salinity loggers (Solinst Levellogger® 5 LTC) were placed in groundwater standpipes in distinct vegetation communities, one each in the Sarcocornia and Juncus communities. The standpipes were PVC pipes of 5 centimetres diameter, sunk into the marsh surface, to a depth of ~120 centimetres. The loggers were attached to a thin rope which was fastened to the top of the standpipe, allowing the loggers to hang 100 centimetres below ground-level, not the top of the pipe. The pipe was capped and sealed with tape to ensure no rainfall directly entered the pipe. Two additional standpipes were deployed on the 4th of May. These were deployed in the same manner as the existing two. One was placed into the Phragmites community, and the other into a stand of Melaleuca trees at the end of the transect. Data was downloaded from the loggers upon subsequent trips to the site.

Figure 5.1: Photograph of the initial eddy co-variance tower set up. The table in the lower-left corner holds the solar panel and battery use to power the tower.

5.1.2. Eddy-Covariance Towers

Initially, only a single eddy-covariance Tower (EC Tower) was deployed on the first visit to the site – 22nd of February. The EC system in use is an IRGASON® Integrated CO_2/H_2O Open-Path Gas Analyser and 3D Sonic Anemometer system that reports fluxes of both CO_2 and water vapour in the air using mid-infrared light (Campbell Scientific, 2020). The field set-up consists of two parts. The first is the tower which holds the measurement equipment – the open-path sensor, the anemometer which measures wind speed and direction in three vectors, and a probe which measures humidity and temperature, as well as the data processing and storage unit. The second part holds a solar panel and a battery supported on a trestle table that powers the equipment on the tower. Power equipment was strapped to the table, also in turn tied to the ground (Figure 5.1). The tower was placed at the junction of the Sarcocornia and Juncus communities (36° 18' 34.12" S, 150° 7' 11.01" E). This placement was designed to capture gas fluxes from either community, dependent on the wind direction, by orienting the Gas Analyser and Anemometer to an Azimuth of 135°. Azimuth alignments were made to perpendicular to the primary wind directions. The gas analyser put at a height of 1.10 metres. On the second visit on the 4th of May, a second EC Tower was deployed, this time placed in the approximate centre of the Juncus community (36° 18' 32.59" S 150° 7' 11.78" E). The Gas Analyser and Anemometer were oriented in a 160° Azimuth. The tower was set-up in the exact manner as the initial tower, except for the instrument height – 1.70 metres. Additionally, the initial tower was deployed on the first visit was moved into the Sarcocornia community (36° 18' 34.83" S   150°   7' 10.33" E). In its new position the sensing equipment was oriented along an Azimuth of 135° and the instrument height was 1.25 metres. The towers were placed in these altered locations to better capture gas fluxes that are attributable to whole vegetation communities at all times, rather than one community or another based on wind direction, as in the first case.

5.2. Field Sample Collection

5.2.1. Soil Samples

Soil samples were collected on each visit to the study site. Samples were collected along the pre-established transect, in the middle of the mudflat, each vegetation community and in February, the transitions between communities in order to detect any shift in the measured environmental variables. Samples were collected using a modified plastic 60 mL syringe with the narrow end cut off to create a tube that could be inserted into the marsh surface to extract a miniature soil core and dispel it into a specimen container. Soil cores were taken to be 5 cm in depth. At each sampling point, a PVC pipe was stuck into the ground to mark the position for return sampling. Five samples were taken at each location, one at the pipe, and then four in a sequence taken from one metre away from the pipe, beginning on the left-hand side, when facing the landward end of the transect (Figure 5.2).
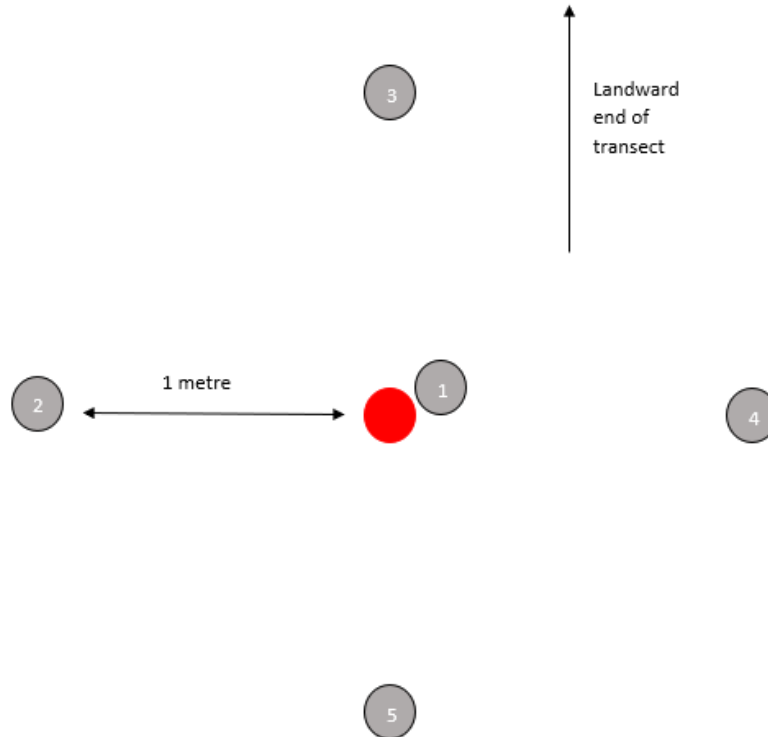
Figure 5.2: Schematic diagram showing the soil sampling procedure. The red circle indicated the PVC markers, and the grey circles represent the sequence of soil samples taken to maintain consistency

Specimen containers were labelled with the respective vegetation community and sequential number. Upon subsequent sampling trips, boundaries between communities were no longer sampled. This decision was made due to the time required to collect the samples, process and analyse them in the lab, and the lack of variance in the measured parameters between one community and the boundary.

5.2.2. Water Samples

Water samples were collected from both the groundwater standpipes and the lake surface on each sample trip (the Phragmites and Melaleuca standpipes were not installed in February and hence were not collected). Twelve samples were taken from each of the two established standpipes, six from the surface of the groundwater and six from the deep end of the pipe. Of these, three 'surface' and three 'deep' samples were also filtered using 45 µm filters to removed dissolved solids and any larger organic matter. This sampling methods was repeated to sample lake surface water, and water from the mouth of Tilba Lake, for comparison of parameter trends.

Upon the second sampling visit in May, the above method was repeated for the lake surface, existing standpipes, and the new standpipes in the Phragmites and Melaleuca communities. Water was also collected from Mystery Bay Beach, to act as a seawater reference against the collected groundwater samples.

5.2.3. Biomass Samples

On the second trip to the study site, samples were also collected to allow for above-ground biomass determination. A 0.25 metre-square quadrat was randomly placed on the marsh surface in the Sarcocornia, Juncus and Phragmites communities. Using secateurs, plant material was removed at ground level and stored in a garbage bag in a cool room until processing. This process was repeated in three locations for each of the Sarcocornia, Juncus and Phragmites communities.

5.3. Laboratory Sample Analysis

5.3.1. Soil Samples

Wet samples were weighed to a precision of 0.01 g and using the known volume of the syringe used to collect them, the wet bulk density was calculated. Samples were then dried at 45°C until constant weight, after which samples were weighed and their dry bulk density and moisture content calculated. Once dried, the samples were ground using a mortar and pestle, and put through a 2-millimetre sieve to separate larger organic matter. Any separated larger organic matter was placed into a separate tray and weighed, then discarded. This weighed component was subtracted from the dry weight total before the calculation of moisture content. Inorganic material caught in the sieve was returned to the sample and they were stored for further analysis. The equipment was rinsed and dried between samples. Samples taken from the Sarcocornia community in February were misplaced between the field and lab, and hence weren't able to be processed and included in the data.

A sub-sample of each ground sample was separated into a centrifuge tube for testing of soil pH, conductivity, and other parameters. Soil was weighed to a precision of 0.0001 g and approximately 5 g of soil was transferred into the tube. The tube was filled distilled water to the mass required for a five to one dilution. Diluted samples were then shaken using an orbital shaker for 24 hours and tested using a Mettler-Toledo Seven GoDuo Water Quality Probe.

Another sub-sample of the dried soil sample was subjected to Loss on Ignition (LOI). Crucibles had been drying beforehand in a 45°C oven. Crucibles were weighed to a precision of 0.0001g, noting the weight. Approximately 2.5 grams of sample was transferred into the crucible and final weight noted. A muffle furnace was used for LOI, and samples were heated at 550°C for four hours as per Heiri, Lotter and Lemcke, (2001). Once cooled, samples were removed from the furnace into a desiccator and then re-weighed to a precision of 0.0001 g. Soil samples were disposed, and crucibles washed and re-dried for subsequent furnace runs.

5.3.2. Water Sample Analysis

Where possible, water samples were filtered in the field, as described in section 4.2.2. Any bulk samples that were brought back to the lab were filtered using the same 45 micrometre syringe filters. The resulting 'surface' and 'deep' samples had both filtered and non-filtered, or 'bulk', components. The Mettler-Toledo Water Quality Probe was used to measure conductivity, salinity, total dissolved solid (TDS) and temperature. A separate benchtop probe (Thermo Scientific Orion Star) was used to measure pH. Each testing probe was also rinsed with distilled water between measurements.

5.3.3. Biomass Sample Preparation

Plant material was separated into species and shortened to appropriate size to fit into foil trays. Material was dried in an oven at 60°C until constant mass, then re-weighed and the final mass recorded. Separation of plant species allowed for species diversity to be determined, as well as overall biomass for the sample area.

5.4. Data Processing

Data from the soil and water results, as well as the water logger data were processed and presented using Microsoft Excel. Averages between all replicates for soil and water data were obtained and their respective standard errors obtained for graphing. Eddy covariance data were pre-processed on Microsoft Excel. Here, appropriate data were selected from the instrument output and refined. EC datapoints had attached data quality flags, ranging from 1 to 9. As per Foken et al., (2012), only classes 1 to 6 were used to carry out analysis on. Any remaining outliers were individually inspected and removed if their associated wind speed or direction, atmospheric stability or friction data were deemed to be non-conforming. EC data were further processed using R-Studio, primarily using the 'openair' package (Carslaw and Ropkins, 2012). This allowed for the creation of windroses, polarplots and boxplots. When separating outputs into day and night datasets, daytime was made to be between 7AM and 5PM, and night-time between 5PM and 7AM. This split was decided based off approximations of sunrise and sunset data from Sydney weather stations.

5.5. Map Making

The maps shown in Figures 4.1 and 4.2 were created using ArcMap software. The vegetation communities and equipment locations shown in Figure 4.2 were identified and mapped using RTK GPS (Trimble R8S) points and vegetation data provided by Dr Michael Hughes from DPIE.

6. Results

6.1. Tidal inundation trends

Figures 6.1 shows the water level relative to Australian Heigh Datum (AHD) for each of the three initial water logger sites. However, the tidal channel logger was deployed much later than the Sarcocornia and Juncus loggers. Figure 6.2 shows the comparison of water levels between the duration of sample collections in February and May. The longer timescale represented by figure 6.1 shows at least one large closed ICOLL phase for Lake Tilba. This is the large peak in water depth occuring towards the end of December 2020. The sudden drop in water level – almost a metre over approximately one hour – was triggered by the reopening of Lake Tilba to the ocean on the 2nd of January 2021, an event that has been confirmed by local landholders. The shorter timescale represented by Figure 6.2 allows a tidal signature to more easily be seen through the short, regular peaking and subsiding of the water depth signature. However, the lack of a tidal signature in the water channel logger is not necessarily indicative of a closed ICOLL phase. Figure 6.2 shows that even though there is no tidal signature in the tidal channel, it is still present in the groundwater.The ground elevation of the initial EC Tower has been included in Figures 6.1 and 6.2 for reference, as it was the only tower deployed during the same time period. Figure 6.2 shows that the water level does sometimes rise to the same elevation as the EC tower, and may affect the flux arising from the footprint around the tower. Although, these effects won't be detected as EC data analysis was conducted on data from the two towers post relocation in May. Individual logger plots, with rainfall data are presented in Appendix Figure 10.1 to 10.3.
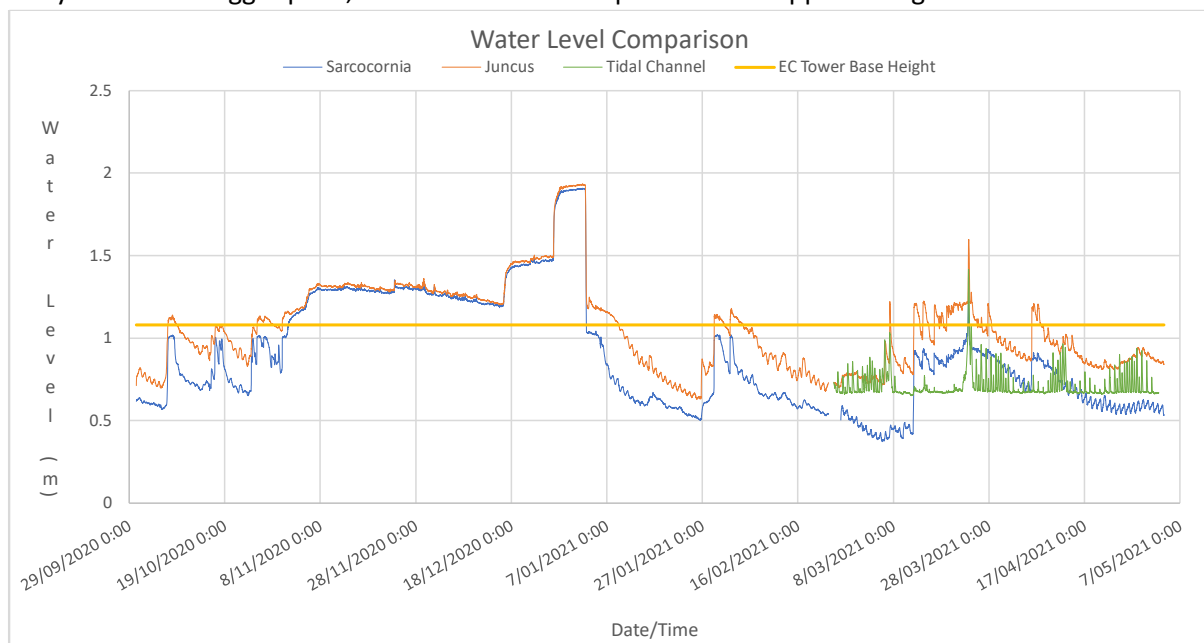
Figure 6.1: Displayed here is the output of all three water loggers overlain against one another. Level is relative to AHD. Also included here for reference is the base height of the initial eddy covariance tower.
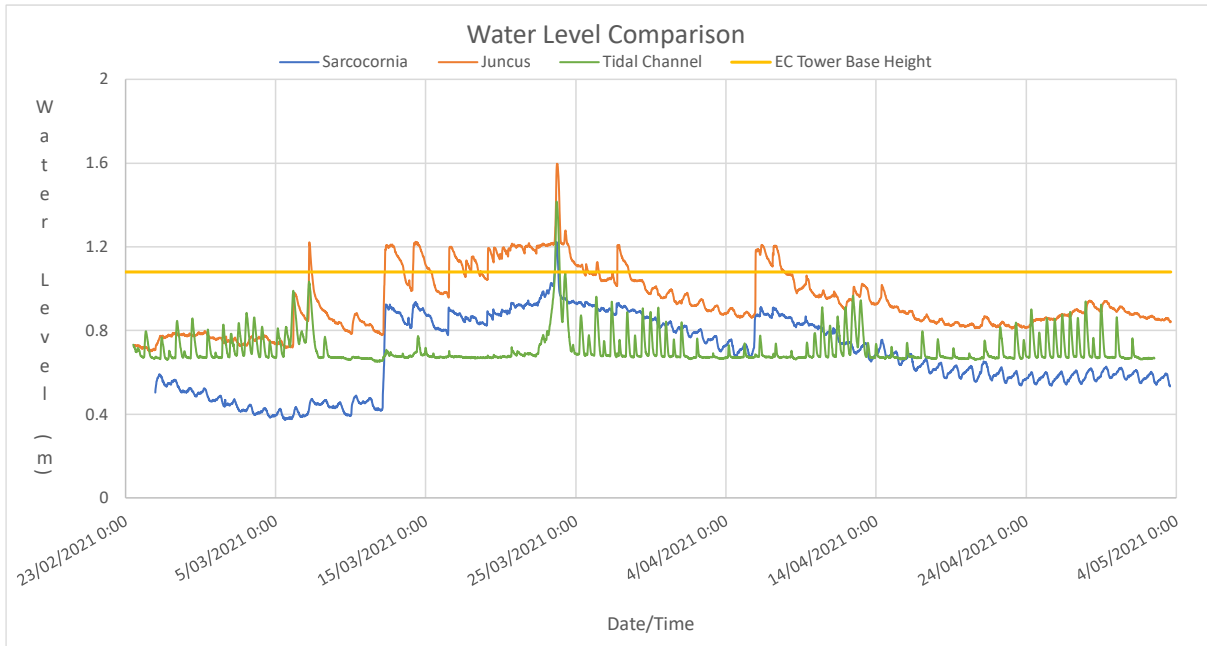
Figure 6.2:Inset of Figure 6.1 to enlarge the period between sample collections where data from all three loggers exists. Here, smaller fluctuations in the water depth are more easily discerned.

6.2. Soil Sample Analysis

6.2.1. Bulk Density

Figure 6.3: Average dry bulk density for each vegetation community, a) from Februrary, including community boundary zones, and b) from May. Values are averages of five replicates and the error bars represent ± standard error.

Soil dry bulk density (DBD) values are shown in Figure 6.3 from samples obtained during the first collection in February were overal much higher than the densities from samples collected in the second collection in May. However, the trend of decreasing DBD from the channel to the upper end of the transect is consistent between both sampling periods.

36

6.2.2. Moisture Content

Average soil moisture content values are shown in Figure 6.4, which shows similar trends over both sampling periods, being a larger moisture content in the mudflat, dropping off and then slowly rising through the transect, with the Melaleuca and Phragmites communities having the highest moisture contents in both cases. Analysis via t-test of the moisture contents of the Sarcocornia and Juncus communities' samples from May yields a P value of 0.001. When using a 95 percent confidence interval, this is substantial enough to reject the null hypothesis and conclude that there is a significant difference between the mean moisture content of both vegetation communities.

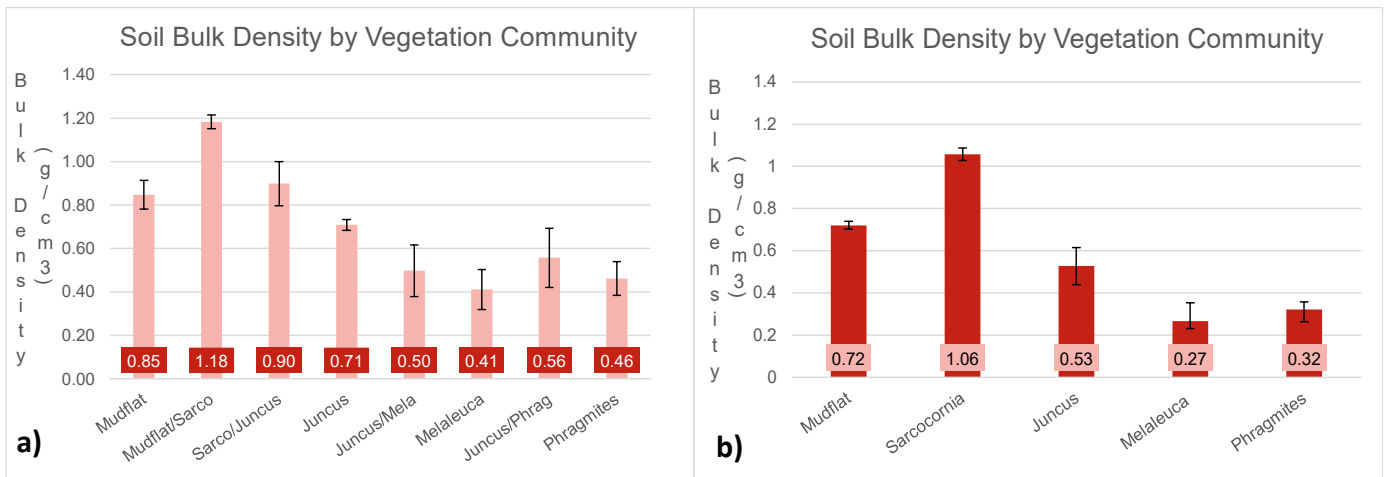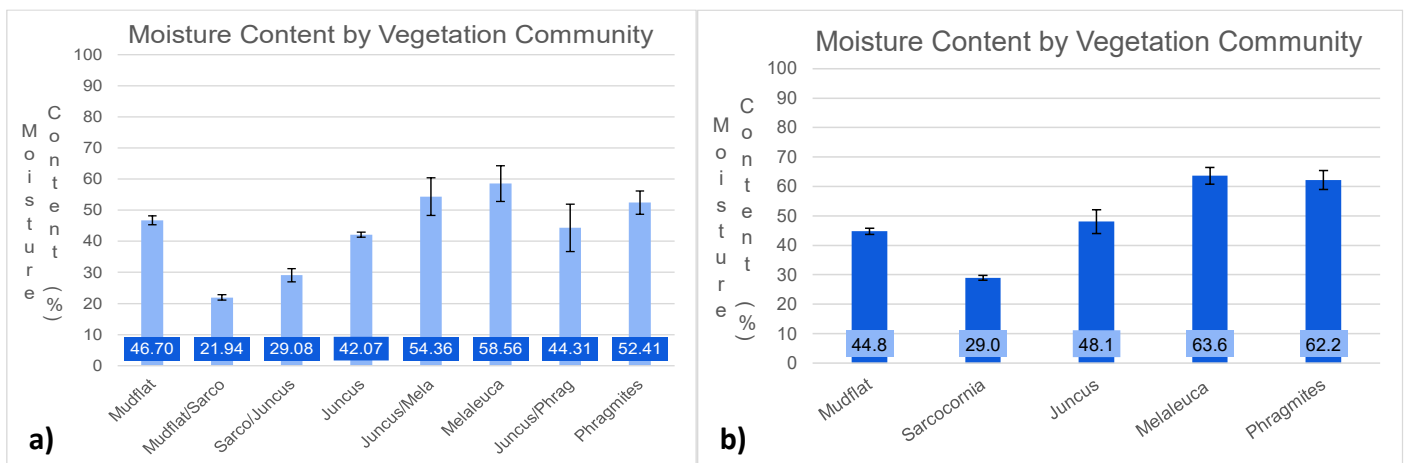Figure 6.4: Moisture content as percentage weight for vegetation community, a) from February, including community boundary zones, and b) from May. Values are averages of five replicates and the error bars represent ± standard error.

6.2.3. Soil Salinity

All salinity values seen in Figure 6.5, aside from the Melaleuca community were lower in samples collected in May than those obtained in February. While the decrease in salinity from the second batch of samples does not coincide with any recent rainfall event seen in Appendix Figures 1.01 to 10.3, there may have been localised rainfall at Lake Tilba that wasn't captured in the Narooma rainfall data. However, rainfall events occurring earlier during March could be influencing soil salinity for an extended period of time, and this combined with reduced inundation events could be responsible for the decline in soil salinity. Alternatively, this could be a return to an open-entrance state representative of an open-ICOLL phase, as the closed phase seen in the lead up to the beginning of January could have elevated soil salinity to the levels shown in Figure 6.5a. t-test analysis of the Sarcocornia and Juncus communities' samples from May yielded a P-value <0.05, confirming that the two communities had significantly different salinities. Conducting a paired t-test of the Juncus Community samples in February and May yielded a P-value of 0.08, which is not enough to reject the null hypothesis, therefore there is no significant change in the Juncus community's salinity between sampling events.

Figure 6.5: Soil Salinity in each vegetation community for a) from February, including community boundary zones, and b) from May. Values are averages of five replicates and the error bars represent ± standard error. Values are final after correction for dilution.

6.2.4. Soil Organic Matter Content

Organic matter (OM) shows consistently higher percentages towards the upper end of the transect in samples retrieved in February (Figure 6.6). Data collected on both occasions shows a smaller OM percentage near the tidal channel at the beginning of the transect that increases along the profile, with a slight decrease in the Phragmites community. There was also increased variability among replicates from February samples. T-test analysis of the Sarcocornia and Juncus communities' samples from May yielded a P-value of 0.049 at a 95% confidence level, confirming that the two communities had significantly different OM percentages. Conducting a paired t-test of the Juncus Community

samples in February and May yielded a P-value of 0.7, which is not enough to reject the null hypothesis, therefore there is no significant change in the Juncus community's OM percentage between sampling events
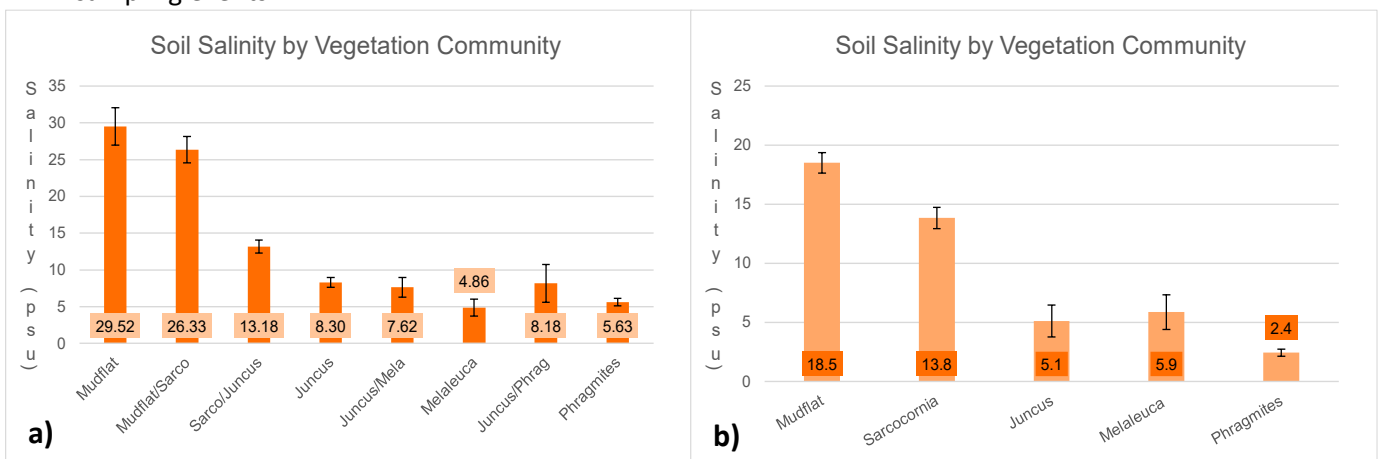

Figure 6.6: Average organic matter content in g/cm³ a) from February, including community boundary zones, and b) from May. Values are averages of five replicates and the error bars represent ± standard error.

Carbon density shows an increasing trend away from the tidal channel in the samples collected in February, but there is an overall decreasing trend away from the channel in May samples (Figure 6.7). Two sites (mudflat and Sarcocornia) show much higher peaks in May samples than their counterparts in February, (albeit comparing Sarcocornia to the boundary samples either side), and the remaining sample sites. T-test analysis of the Sarcocornia and Juncus communities' samples from May yielded a P-value <0.05, confirming that the two communities had significantly different carbon densities. Conducting a paired t-test of the Juncus Community samples in February and May yielded a P-value of 0.41, which is not enough to reject the null hypothesis, therefore there is no significant change in the Juncus community's carbon density between sampling events
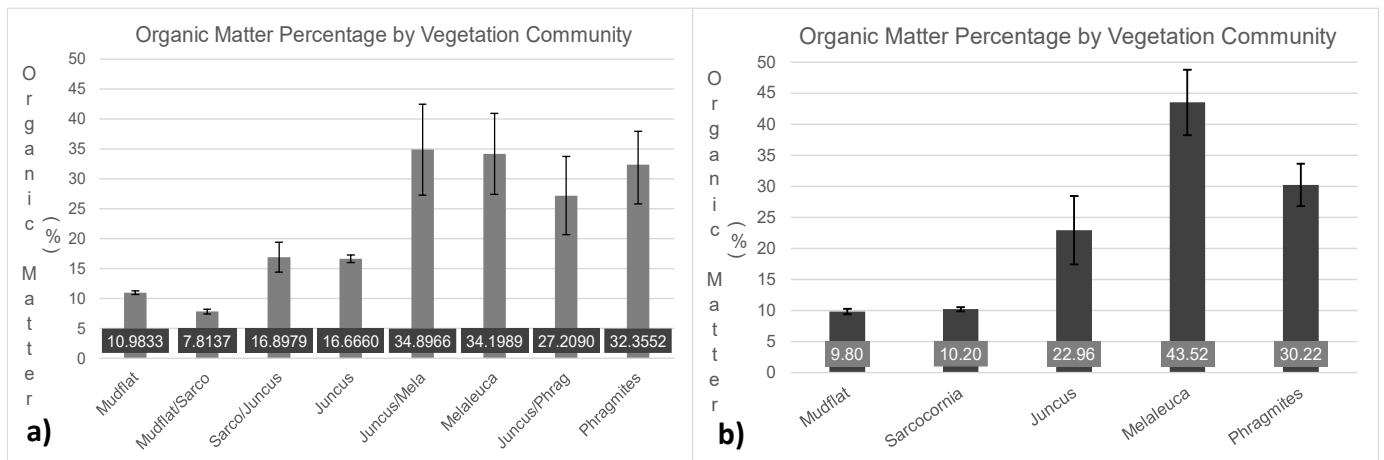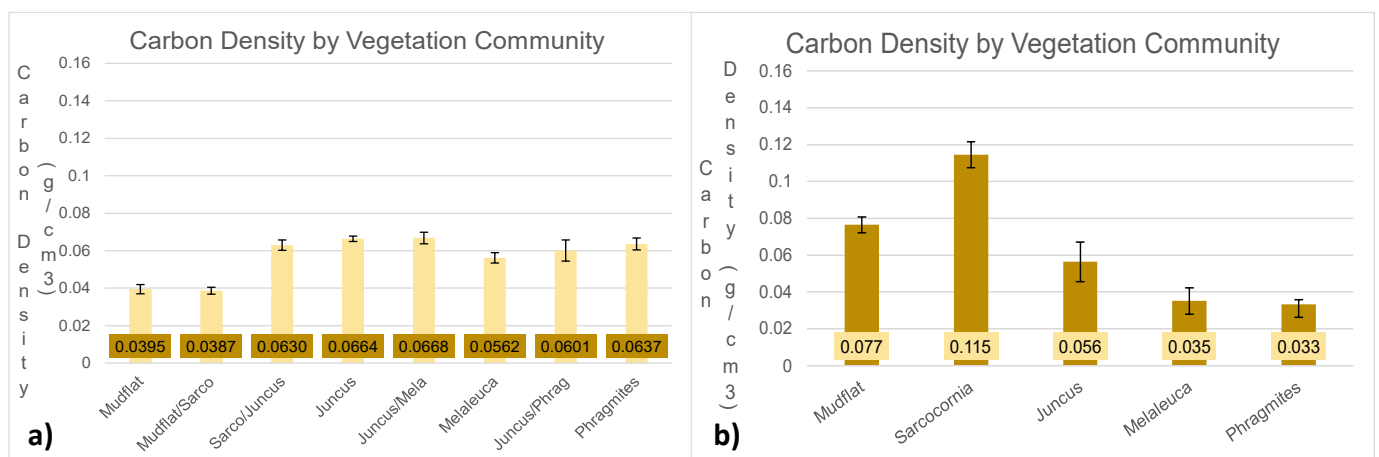

Figure 6.7: Average organic carbon density in g/cm³ for a) from February, including community boundary zones, and b) from May. Values are averages of five replicates and the error bars represent ± standard error.

6.3. pH Results

Overall, the pH values obtained in February showed a much narrower range than those obtained in May. On both occasions, there was an acidity shift from the tidal channel towards the rear of the transect.

Groundwater pH results from February all range between a pH range of 7 to 8, sitting close to neutral. A similar result is seen in the Juncus and Sarcocornia groundwater pH values from May as well. In all cases except the Sarcocornia values from May, the filtered treatments show a more alkaline pH than the bulk samples. The mean ± SE for seawater taken from the open coast was 7.86 ±0.03 and 7.70±0.02 for the bulk and filtered samples respectively. All pH data is shown in Appendix Figures 10.4 to 10.6

6.4. Groundwater Salinity

Groundwater salinity concentrations from samples collected in February are overall lower than the samples collected in May. They had higher associated standard errors, which may be due to more disturbance in the first sample collection (Figure 6.8). The addition of data from the Melaleuca and Phragmites communities in Figure 6.9 shows a very low salinity further away from the influence of the tidal channel. Overall, there seems so be no effect of filtering on the salinity concentrations unlike for the pH data presented in the Appendix.
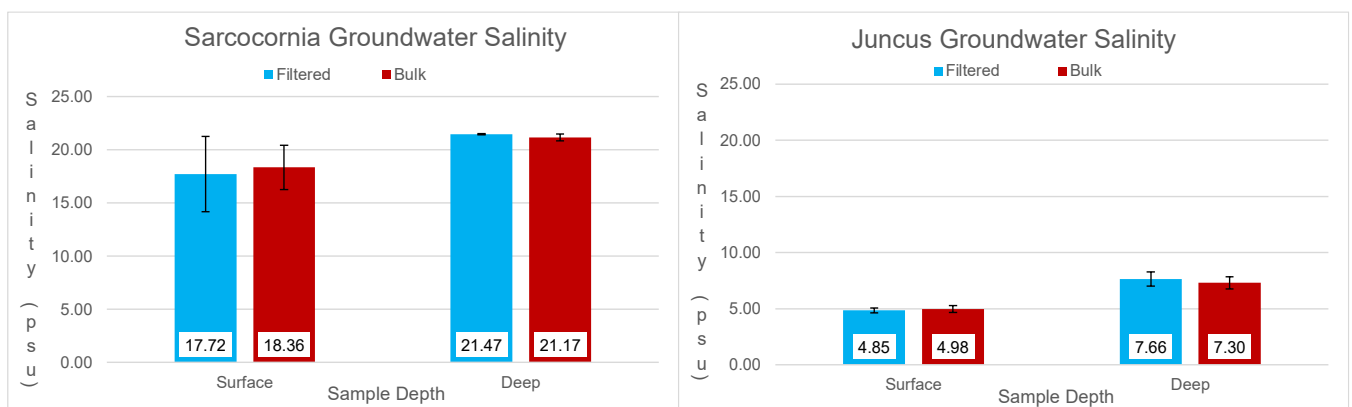

Figure 6.8:Community groundwater salinity results from February samples for the Sarcocornia and Juncus vegetation communities. Values are average salinities from three replicates and are presented as Practical Salinity Units (psu). Error bars indicated standard error.
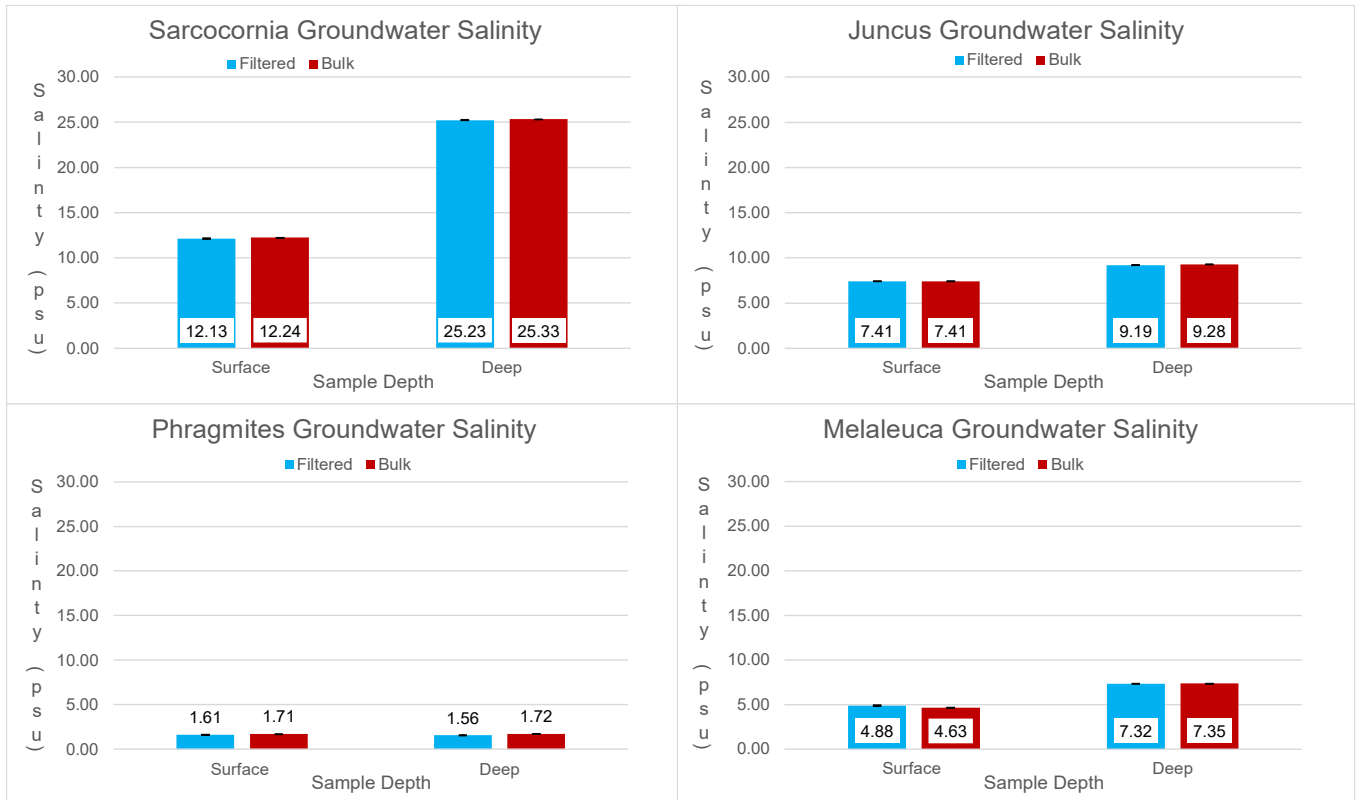
Figure 6.9:Community groundwater salinity results from May samples for all four vegetation communities. Values are average salinities from three replicates and are presented as Practical Salinity Units (psu). Error bars indicated standard error

6.5. Biomass

Vegetation community composition varied between strata. The Sarcocornia community was completely dominated by *S. quinqueflora* and had a mean dry biomass weight of 0.48 ± 0.06 kg m^2, with ranges from 0.37 to 0.54 kg m^2. The Juncus community showed more species of vegetation, however, was still vastly dominated by *J. kraussii* and *S. quinqueflora* (Figure 6.10). The average dry biomass for each vegetation type was 0.28 ± 0.15 kg m^2. The total dry biomass across the Juncus community strata is 1.40 kg m^2. The Juncus community had slightly more variability between replicates, with a minimum biomass value of 0.90 kg m^2, and a maximum of 2.08 kg m^2.

The Phragmites community was dominated by *P. australis*, with lesser contributions from other plant species like *J. kraussii* (Figure 6.11). The average dry biomass for each vegetation type was 0.25 ± 0.13 kg m^2. The total dry biomass across the Phragmites community strata was 0.99 kg m^2, with samples ranging from 0.90 to 1.06 kg m^2. A further breakdown of summary values for each vegetation strata is provided in Table 6.1.

Figure 6.10: Percentage composition of the Juncus vegetation community. Percentages are yielded from averages of dry weight across three replicates.

Figure 6.11:Percentage composition of the Phragmites vegetation community. Percentages are yielded from averages of dry weight across three replicates.
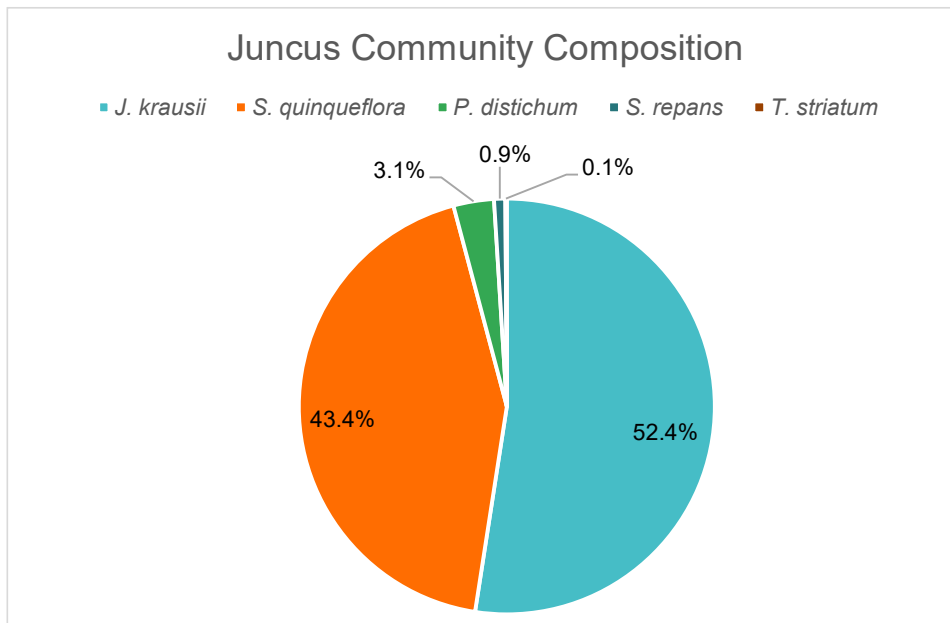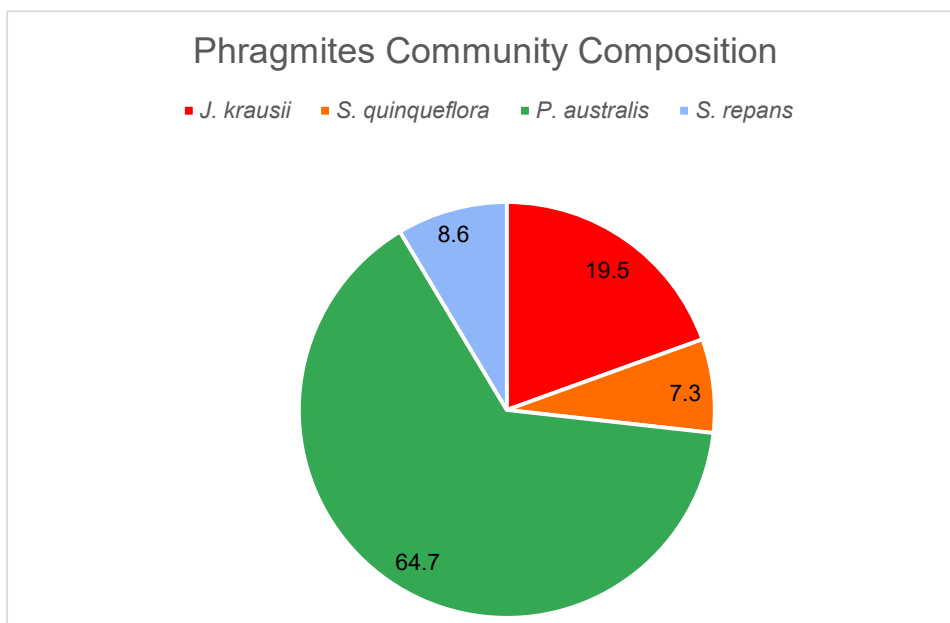
Table 6.1: A breakdown of the summary values for each vegetation community where biomass samples were collected. 'Total Community Biomass' indicates the biomass value when scaled up to the entire vegetation community's area.

				Measured Characteristic			
Community		Dry Weight	MC%	BM%	kg dry/m^2	Standard Error	%Veg by dry Weight
Sarcocornia	S. quinqueflora	1810.16	80.0	20.0	0.480	0.057	100
Juncus	J. krausii	517.13	64.7	35.3	0.690	0.493	52.4%
	S. quinqueflora	428.12	85.8	14.2	0.571	0.162	43.4%
	P. distichum	31.04	67.1	32.9	0.124	0.062	3.1%
	S. repans	8.63	84.5	15.5	0.012	0.009	0.9%
	T. striatum	1.12	86.5	13.5	0.004		0.1%
	Mean Individual BM				**0.280**	**0.146**	
	TOTAL Community BM				**1.400**		
Phragmites	P. australis	479.16	73.7	26.3	0.64	0.168	8.6
	J. krausii	144.22	75.2	24.8	0.19	0.116	19.5
	S. quinqueflora	53.71	85.6	14.4	0.07	0.068	7.3
	S. repans	63.56	83.7	16.3	0.08	0.062	64.7
	Mean Individual BM				**0.25**	**0.133**	
	TOTAL Community BM				**0.99**		

6.6. Eddy Covariance

6.6.1. Background Synoptic Data

6.6.1.1. Temperature

Average, half-hourly temperature readings are largely consistent between both communities, and also between day and night readings between communities (Figure 6.12). The average overall temperatures were 15.5°C and 15.2°C for the Sarcocornia and Juncus communities respectively. Sarcocornia daytime temperatures averaged at 16.5°C and night-time at 14°C, while daytime temperatures for the Juncus community sat at an average of 16.3°C and night-time 13.7°C.

Range of Temperatures for each Community
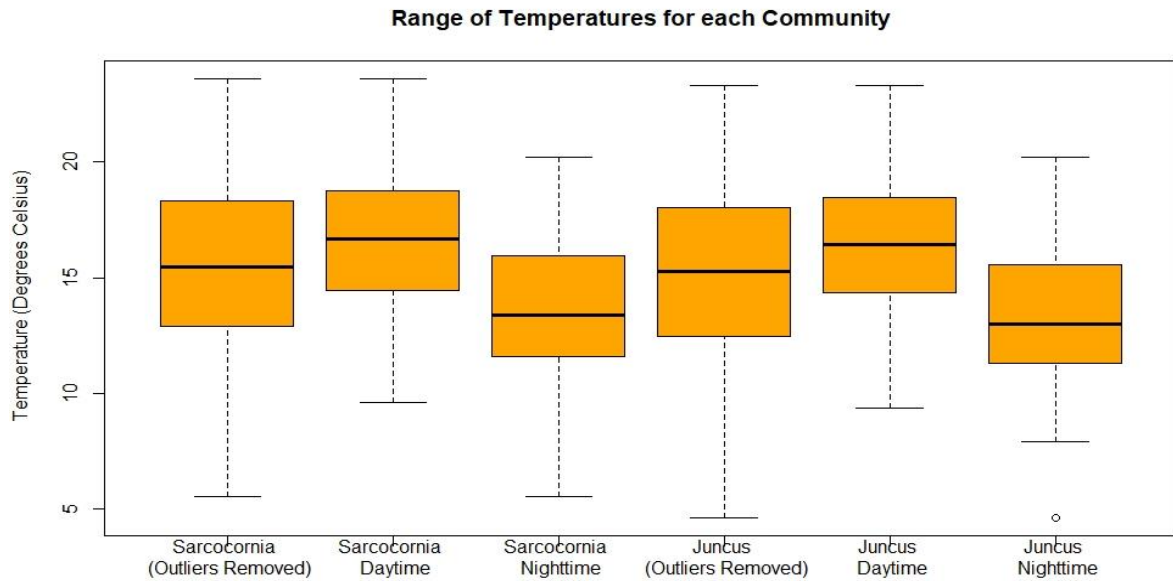
Figure 6.12: Boxplots showing the range of temperature readings for both the Sarcocornia and Juncus communities. Temperature ranges are then separated into daytime and night-time plots for each community.

6.6.1.2. Humidity

Similarly to temperature, humidity data shows little variation between communities, but does show differences within each community between night and day (Figure 6.13). The overall humidity was 66% and 67% for the Sarcocornia and Juncus communities respectively. The former having a 62% daytime and 72% night-time humidity average, while the daytime humidity was 63% and 73% for the night in the Juncus community.

Range of Humidity for each Community
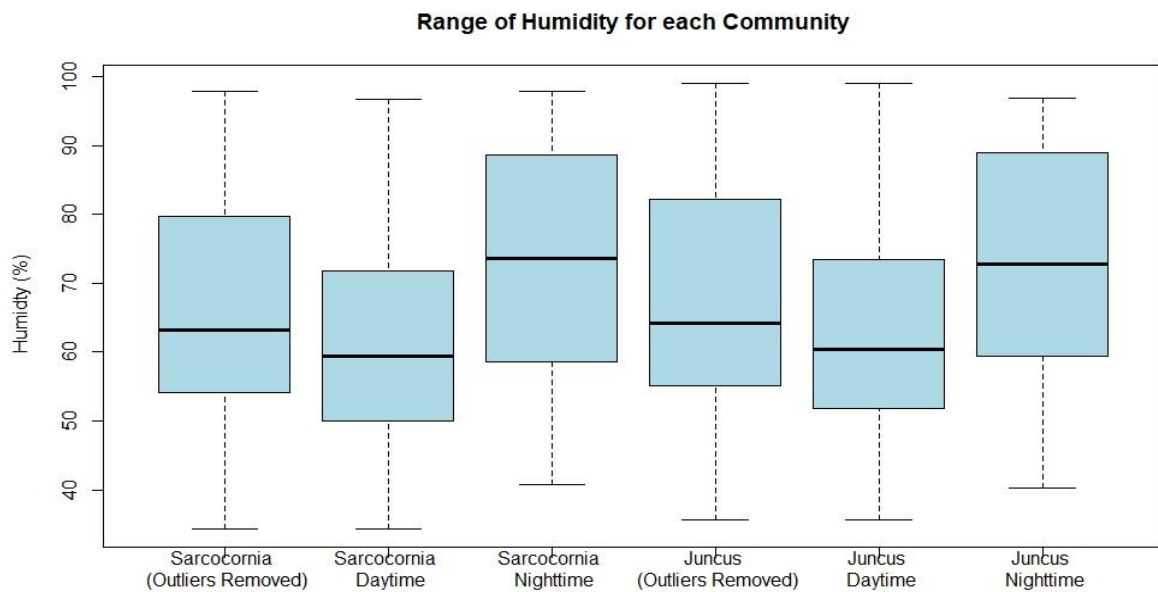
Figure 6.13: Boxplots showing the range of relative humidity measurements for both the Sarcocornia and Juncus communities. Humidity ranges are then separated into daytime and night-time plots for each community.

6.6.1.3. Wind Characteristics
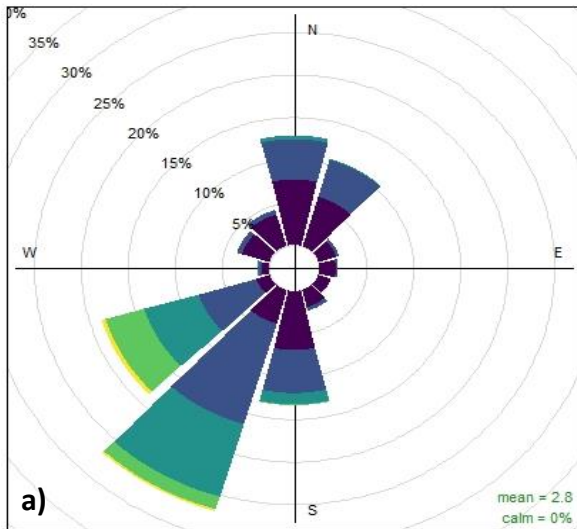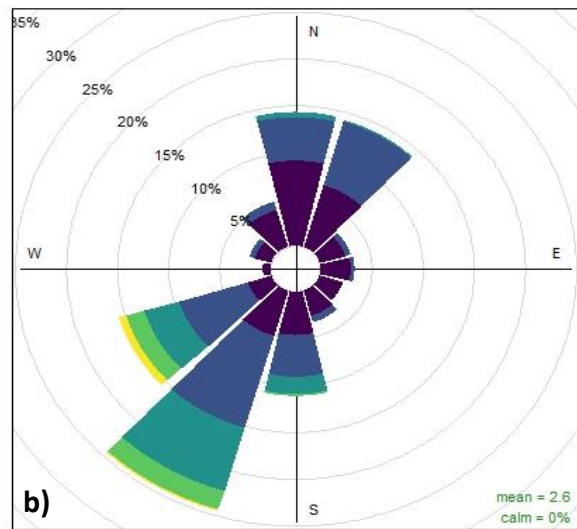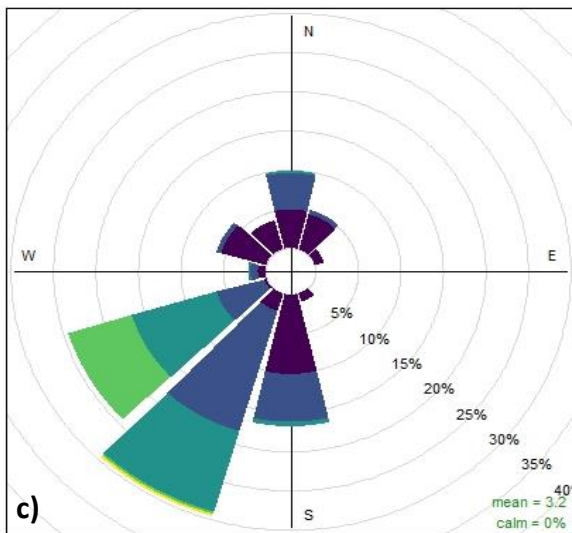
Figure 6.14: Windrose plots from the Sarcocornia EC tower. Each plot shows the frequency (as a percentage) of a measurements wind direction and its associated speed. a) shows the overall wind data and b) and c) show the split into daytime and night-time datasets respectively.

Figure 6.14a shows that a majority of the EC tower measurements are associated with wind coming from the south-west, with a lesser influence from the north and north-north-east. The northerly and north-north-easterly influence becomes slightly more pronounced when looking at daytime measurements only. The daytime maximum speed was measured at 9.6 m s^{-1}. Overnight, the number of measurements originating from northerly sources drops from between 5 and 10 percent of the total count. The night-time measurements also show more measurements falling into the 6 to 8 m s^{-1} category than during the day, but there is only a maximum wind speed of 8.3 m s^{-1}.

Unlike in the Sarcocornia community, the Juncus EC tower recorded the majority of its measurements with a south-westerly or southerly wind direction (Figure 6.15). Regardless of time of day, the maximum windspeed reached was 8 m s^{-1}, although this was more common during the day. The daytime measurements also contain more counts with a wind speed less than 2 m s^{-1} than the night.
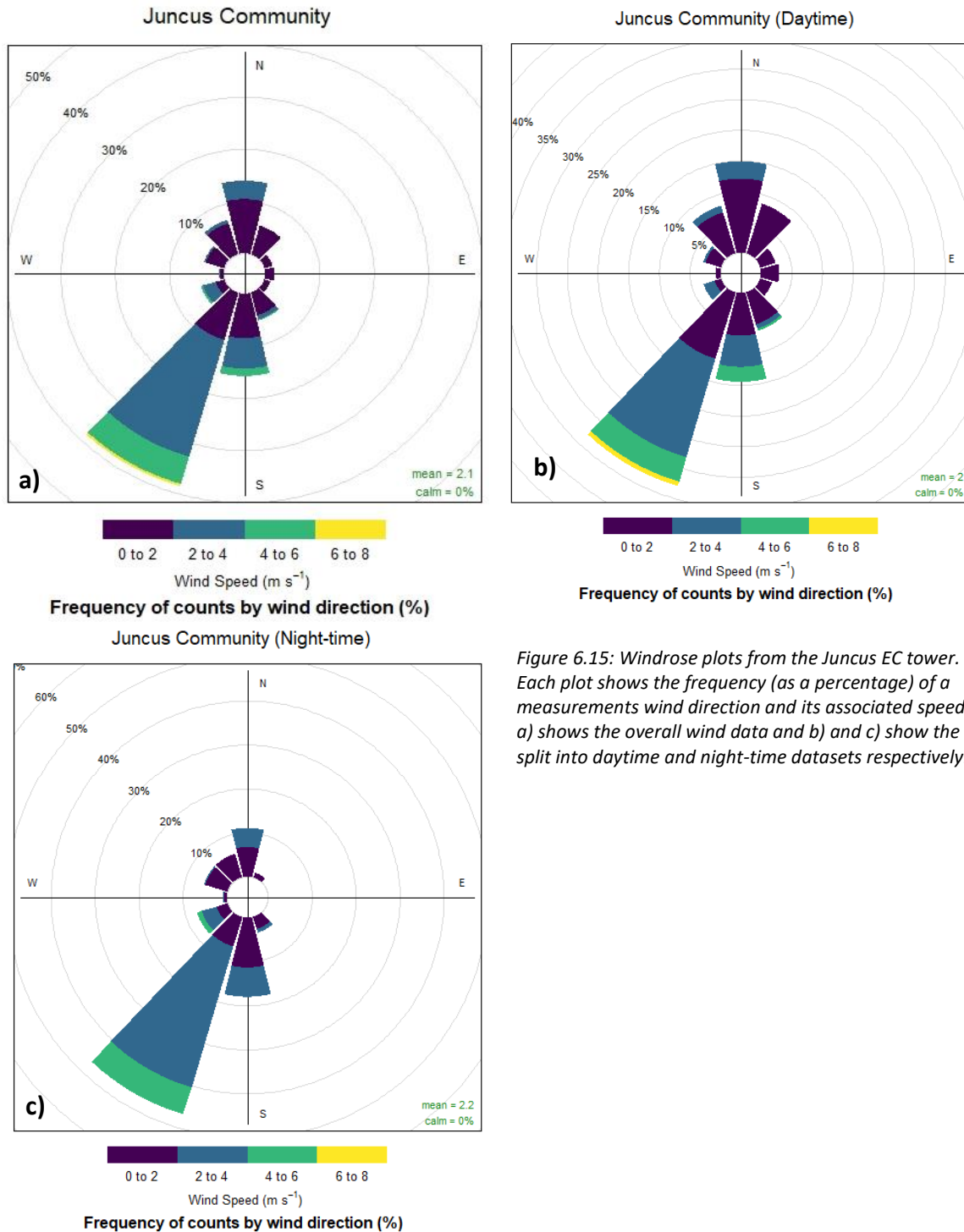
Figure 6.15: Windrose plots from the Juncus EC tower. Each plot shows the frequency (as a percentage) of a measurements wind direction and its associated speed. a) shows the overall wind data and b) and c) show the split into daytime and night-time datasets respectively.

6.6.2. Carbon Dioxide Flux

When comparing the overall flux of the two vegetation communities, the Juncus community has stronger positive and negative fluxes than the Sarcocornia community (Figure 6.17). Both communities have the maximum flux contribution arising from air parcels within 20 metres of the respective EC Tower (Figure 6.16). However, the Juncus community tower does receive maximum flux contributions from a wider array of directions.

When the flux data is separated into daytime and night-time, difference are more easily discerned. Both communities exhibit primarily negative fluxes during the day, but this effect is stronger in the Juncus as seen in Figure 6.18b. When the night-time flux data is separated, as in Figure 6.19, both vegetation communities show a strong positive flux with wind directions coming from the east, with that arising from the Juncus community being much greater than that from the Sarcocornia.
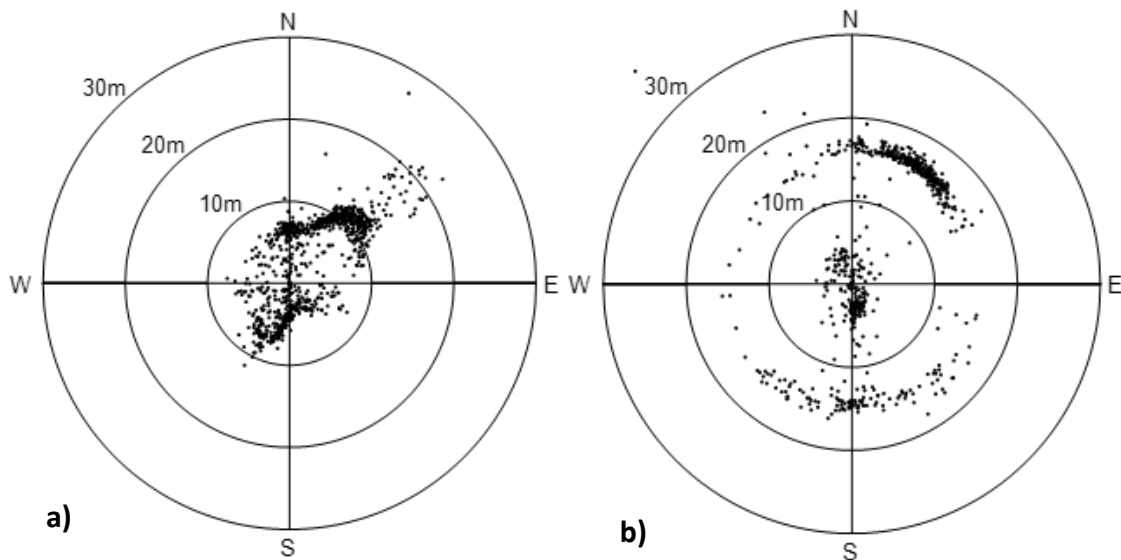
Figure 6.16: Footprint plots detailing the distance and direction of each EC flux measurement for a) the Sarcocornia community and b) the Juncus Community
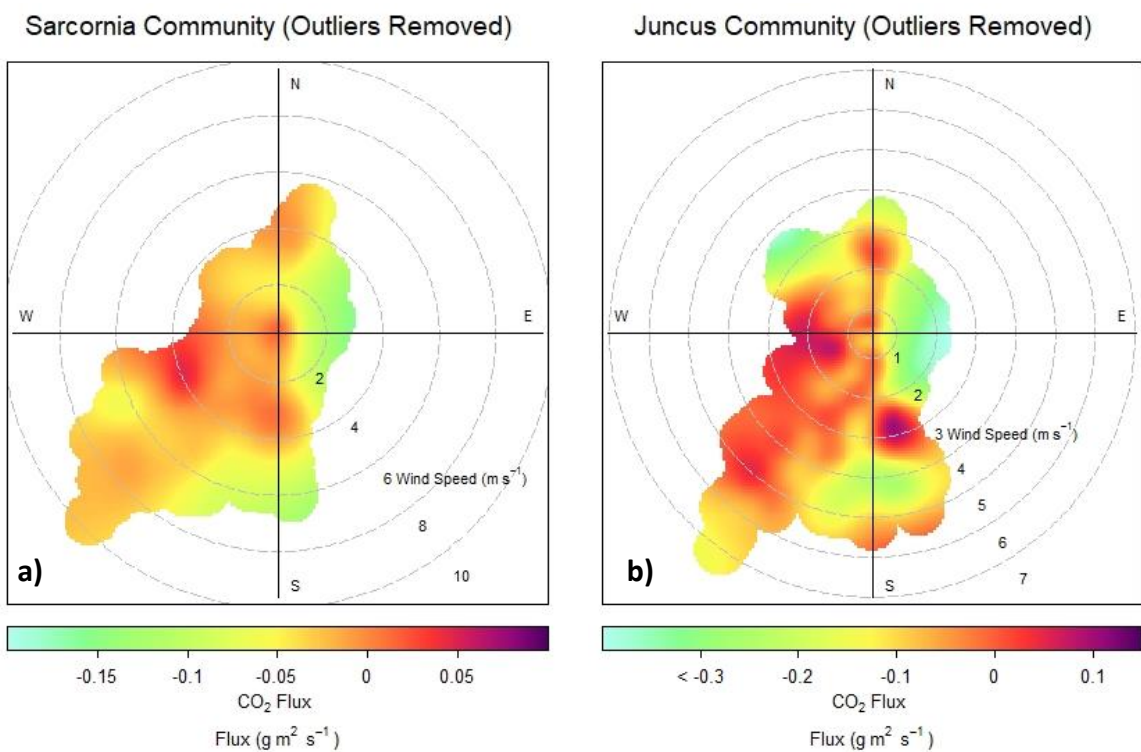
Figure 6.17: Polar plots of the overall average flux from a) the Sarcocornia community, and b) the Juncus community. Fluxes here are plotted using wind speed and direction.
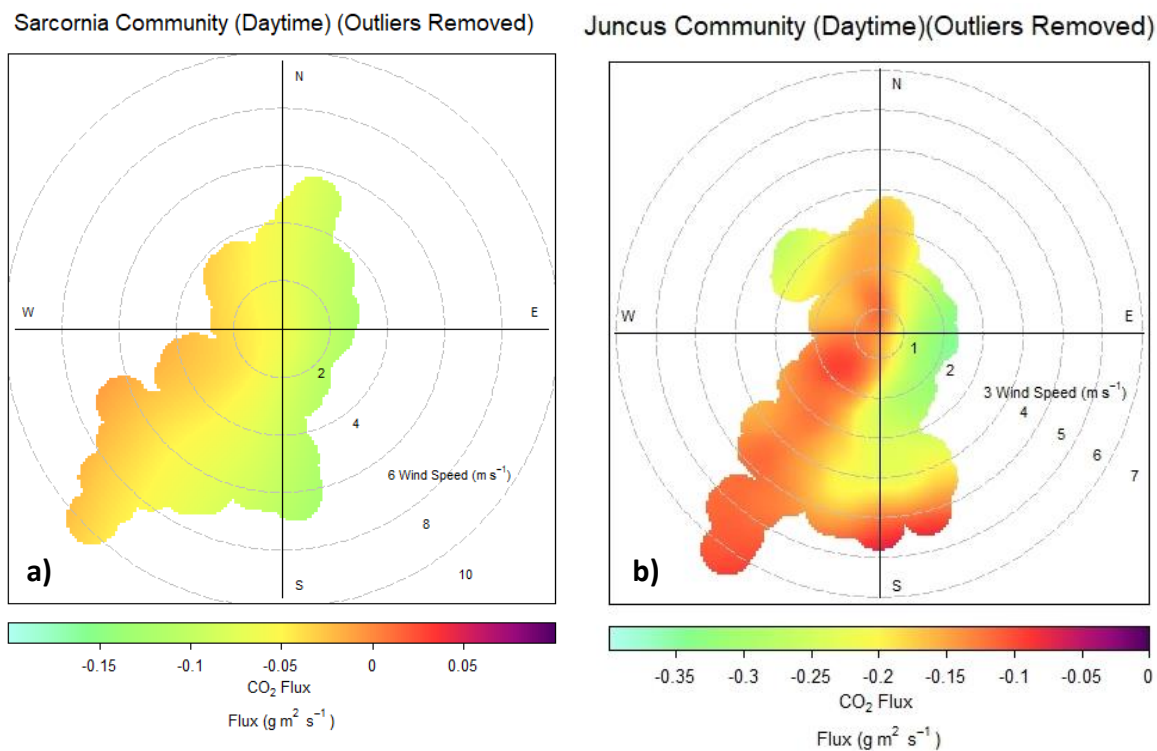
Figure 6.188: Polar plots of thedaily daytime average flux from a) the Sarcocornia community, and b) the Juncus community. Fluxes here are plotted using wind speed and direction.

48
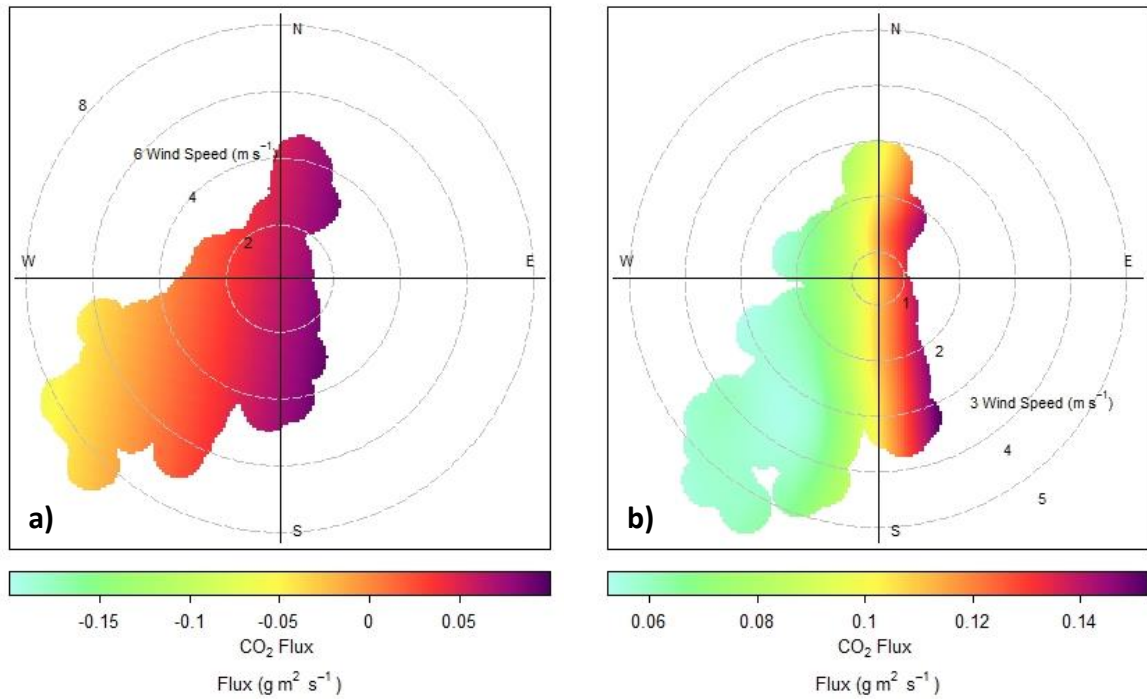
Figure 6.199: Polar plots of the daily night-time average flux from a) the Sarcocornia community, and b) the Juncus community. Fluxes here are plotted using wind speed and direction.
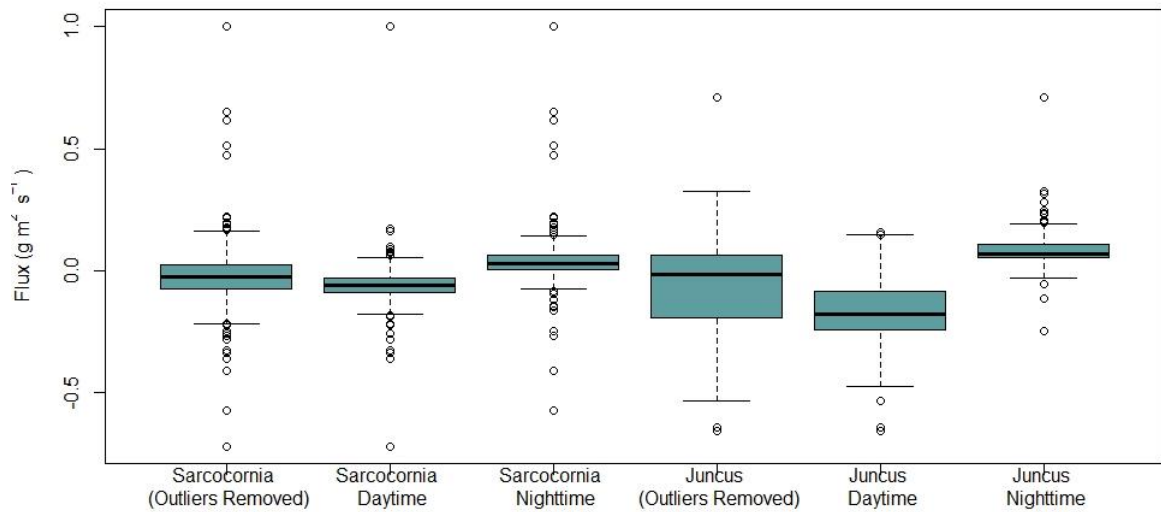
Figure 6.20: Boxplots showing the range of flux readings for both the Sarcocornia and Juncus communities. Flux ranges are then separated into daytime and night-time plots for each community.

Figure 6.19 has been included to show the range of half-hourly flux measurement for each community, and further decomposed into their respective daytime and night-time datasets. It further reinforces the stronger flux values on both the positive and negative ends of the scale for the Juncus community.

Statistical analysis of the mean daily flux values using a Welch Two Sample t-test, yielded a P-value of 0.003. Using a confidence interval of 95%, this result is enough to accept the alternative hypothesis that there is a statistically significant difference between the mean daily flux of both the Sarcocornia and Juncus vegetation communities. The same result was found when comparing the mean daily daytime flux, however, this P-value was much smaller than 0.05. No statistically significant difference was found when applying the t-test to the average daily night-time flux (P=0.136). Means for each vegetation community in differing time-of-day splits are displayed in Table 6.2.

Table 6.2: Mean CO_2 fluxes with associated standard error for each community, including the mean daily flux, daily mean daytime flux and daily mean night-time flux.

	Sarcocornia Community Flux Mean ± SE (mg CO_2 m^{-2} s^{-1})	Juncus Community Flux Mean ± SE (mg CO_2 m^{-2} s^{-1})	P-Value
Overall	-0.029 ± 0.0062	-0.078 ± 0.013	0.003
Daytime	-0.061 ± 0.0046	-0.162 ± 0.013	<0.001
Night-time	0.053 ± 0.0178	0.096 ± 0.0069	0.136

7. Discussion

7.1. Differences in Carbon Dioxide Fluxes

Net fluxes of CO_2 from the Juncus community were significantly more negative at a 95% confidence interval, than those from the Sarcocornia community. When the night-time flux data were removed, there was an even greater negative flux of CO_2 in the Juncus community during daytime hours. One driving factor of this difference may be the Juncus community having a much higher average biomass than the Sarcocornia community. Having a larger biomass – more than triple – it would be expected that the Juncus community draws down much more CO_2 than the Sarcocornia community (Emery and Fulweiler, 2014; Moseman-Valtierra *et al.*, 2016). This is reflected in the Lake Tilba data, both when comparing the Net Ecosystem Exchange (NEE) of each community, and the total annual amount of carbon sequestered by a kilogram of dry biomass (Table 7.1). Combined, the Lake Tilba saltmarsh flux is -385 mg C m^2 hour, a value in which is higher than the 35 – 207 mg C m^2 hour^{-1} saltmarsh fluxes reported by Livesley and Andrusiak, (2012).

Table 7.1: Community data for the two monitored vegetation communities.

Vegetation Community	Area (m^2)	Measured Biomass (kg dry m^{-2})	Total Community Biomass (kg)	Mean Hourly Flux (mg CO_2 m^{-2} hour^{-1})	NEE (g C m^{-2} year^{-1})	C sequestered (g C kg^{-1} BM)
Sarcocornia	794	0.48	381.12	-104.4	-68.90	-0.27
Juncus	514	1.40	719.6	-280.8	-568.40	-0.39

However, when comparing NEEs from the Lake Tilba saltmarsh in Table 7.1 with values obtained from the literature in Table 3.3, there is a large disparity. NEE values for the Sarcocornia community are less negative than the -179 g C m^{-2} year^{-1}, obtained by (Forbrich, Giblin and Hopkinson, 2018). However, when accounting for the season that data exist from, the NEE of the Sarcocornia community sit within the range of values reported in a Northern Hemisphere peatland (-60 g C m^{-2} year^{-1}) (Peichl *et al.*, 2014).

NEE values from the Juncus community exceed the magnitude of those reported in Table 3.3, up to three times. When comparing the Juncus community to communities of *Spartina alterniflora* in the Northern Hemisphere, values from Tilba Lake still outweigh the magnitude of NEE by approximately two times for the same season (Zhou *et al.*, 2015).

As, flux data was collected was collected during autumn, they may underestimate the NEE of the ecosystem, as CO_2 fluxes may be even more negative during their growing seasons in spring and early summer (Emery and Fulweiler, 2014). Hence, monitoring over annual timescales is necessary to determine the true NEE, but also how the Lake Tilba saltmarsh may compare to other locations.

The Juncus community is located further away from the source of any tidal influence, and hence, may be less prone to inundation and salinity stresses, allowing more opportunity for growth and carbon sequestration. The Juncus community consistently has a lower soil salinity (8.30 and 5.1 psu), than the Sarcocornia community, and in May, this difference was significantly different. As an increase in salinity can have an inhibitory effect on carbon mineralisation, it is logical that the Sarcocornia would have a lower flux (Doroski, Helton and Vadas, 2019; Luo *et al.*, 2019). The current location of the Juncus community within the tidal frame may not remain unchanged, due to Lake Tilba being an ICOLL. As evidenced by Figure 6.1, closed ICOLL phases can significantly inundate the entire saltmarsh, which may act to reduce CO_2 emissions from the marsh, but also drown vegetation if the inundation continues longer than several months, reducing sequestration capacity in the short-term (Naidoo and Kift, 2006; Saintilan, 2009; Livesley and Andrusiak, 2012). During open ICOLL phases, the saltmarsh will be subject to impacts of SLR. With inundation increasing in depth and duration, it is likely that the more salt-tolerant Sarcocornia community, dominated by *S. quinqueflora*, will slowly increase its range over the Juncus community, dominated by the less salt-tolerant *J. kraussii*. Results from Lake Tilba suggest that this occurrence will overall decrease the sequestration capacity of the saltmarsh.

Unfortunately, additional water logger data were not able to be retrieved from the deployed instruments due to travel restrictions imposed by the NSW Government in response to the June Coronavirus outbreak. As a consequence, water level data is not available for the same period as the flux data analysed in this project, hence no relationships or conclusions can reliably be made for an effect of inundation on CO_2 fluxes.

Day-night cycles of respiration also account for variation in CO_2 fluxes in the Tilba Saltmarsh. While the daytime fluxes of both measured vegetation communities are significantly different to one another, they also differ from their respective night-time fluxes. In both communities, night-time fluxes do not, on average, exceed the magnitude of their daytime flux. The night-time fluxes presented in Table 6.2 could be considered the base respiration rates of each community, and the daytime fluxes the net production of each community. This idea further agrees with the data presented in Table 7.1, in that the Juncus community has a higher capacity for carbon sequestration than the Sarcocornia community.

With respect to CH_4 emissions, while direct measurement did not happen as a part of this research project, it may be possible to infer whether methanogenesis is occurring, and where on the saltmarsh CH_4 emissions may arise. As higher salinities can significantly reduce CH_4 emissions, the mudflat and Sarcocornia community may have lower, or even no, CH_4 emissions due to their high salinities, particularly from samples collected in February 2021 (Figure 6.8a) (Livesley and Andrusiak, 2012). The remainder of the saltmarsh may have mixed CH_4 fluxes, as Australian Melaleuca forests have been found to be moderate CH_4 sinks (Livesley and Andrusiak, 2012). Future monitoring of CH_4 at this site would be beneficial, as the monitoring of CO_2 alone may not be sufficient to determine if a wetland is an overall sink or source of greenhouse gases.

7.2. Trends in Environmental Parameters

The distribution of vegetation within the Tilba Lake wetland matches that of other coastal wetlands along the NSW coastline, however with a lack of mangroves. The absence of mangroves within the study site could be due to the nature of the lake being intermittently closed to the ocean, with extended periods of inundation not being conducive to mangrove propagation, or drowning any mangroves that may successfully colonise the area (Saintilan, 2009). *S. quinqueflora* biomass values from Lake Tilba match biomass data obtained by Clarke and Jacoby (1994) (Table 7.2). Similarly, *J. kraussii* biomass data was also consistent with values obtained by Clarke and Jacoby (1994). Additionally, the P. australis community was constrained within a lower salinity part of the wetland, which is typical to the species as described by Saintilan, (2009).

Table 7.2: Biomass data for the Sarcocornia and Juncus communities, comparing values obtained from Lake Tilba with those obtained by Clarke and Jacoby (1994). All values are in g m2. N/R = not reported.

	Min	Max	Mean
Sarcocornia (Tilba)	370	540	0.48
Juncus (Tilba)	90	2080	1.4
Sarcocornia (Clarke and Jacoby, 1994)	52	1184	317
Juncus (Clarke and Jacoby, 1994)	96	4400	N/R

On both sampling occasions, the soil salinity showed a decrease away from the tidal channel, however the salinities were lower on the second occasion, but the Juncus soil salinity did not fall enough for there to be a statistically significant difference. Three scenarios exist as to why this may

be the case. Firstly, as mentioned in section 6.2.3, this drop in salinity throughout the sea-ward end of the transect may be due to a larger amount of time having passed since Lake Tilba reopened to the open ocean, allowing salinity to return to a state that is less representative of constant inundation by concentrated saline water. However, a return to a 'base-line' salinity is not represented in conductivity from the water loggers (Appendix Figure 10.7). Alternatively, this drop in salinity could be due to three large rainfall events that occurred between the two sampling trips, acting to flush salts out of the soil and freshen them. Again, this is not fully represented in the groundwater conductivity data. While there is a drop in conductivity, namely in the Sarcocornia community, this is sustained and not just around the same time as the rainfall events (Appendix Figure 10.2 and 10.3 for rainfall, 10.7 for conductivity). Thirdly, conductivity and groundwater salinity data from the Sarcocornia and Juncus water suggests that the groundwater salinity is not changing between the two sampling periods, indicating that there may not be a return to open-phase salinity conditions. Instead, water level data suggests that when the Lake is closed, both communities exhibit the same level of inundation, but when the Lake is open, the Juncus community groundwater maintains a consistent depth $10 - 30$ centimetres higher than that of the Sarcocornia despite being at a higher elevation (Figure 6.1 and 6.2). A higher groundwater level, and the lower soil and groundwater salinity and logger conductivity indicates that there may be a fresh-to-brackish water lens located underneath the Juncus community. The presence of this fresher lens would provide an explanatory factor for why we find the Juncus community in the location where it is, as it is generally a low salt-tolerant species (Naidoo and Kift, 2006). Although, this does present further implications for SLR, as continued saltwater intrusion may completely intrude over this fresher-water lens, or drastically decrease its size. Removal or reduction of the Juncus community's buffer from the saline water would potentially lead to a mass die-back in the community, with flow-on effects to greatly reduce the sequestration capacity of the entire saltmarsh. Additional groundwater sampling of the Lake Tilba saltmarsh may be beneficial to better determine the extent of this lens, as it may also reach to the Phragmites and Melaleuca communities, which also had a low soil salinity. No logger data is yet available to confirm this hypothesis.

Soil carbon density shows opposing trends between the two sampling dates. In the samples obtained from February 2021, there is an increase in soil carbon density away from origin of tidal influence, with a peak in the Juncus community, and then off the transect in the Phragmites community – two heavier biomass zones. Despite vegetation communities with a higher biomass having the potential to contribute more carbon to the soil, it is likely that this is not the primary driver of carbon density differences (Kelleway et al., 2016a). OM percentage shows a similar trend in the February samples, however the peak now sits in the Melaleuca community. While it cannot yet be inferred from water logger data, the Melaleuca community may be less frequently inundated by tidal

waters due to its elevation within the tidal frame (~1.52 m AHD). Less frequent inundation would likely leave more OM on the wetland surface as it is not transported away by tidal flows (Saintilan *et al.*, 2013). In May samples, carbon densities are greater at the sea-ward end of the transect, while OM percentages are greater towards the land-ward end. In both parameters, the Sarcocornia and Juncus community means are significantly different to one another, but the Juncus community means do not show a significant change between sampling events.

There appears to be a negative relationship in February between carbon density and soil salinity. Yet in the May samples, both soil salinity and carbon density decrease along the length of the transect. As for carbon density, soil salinity values in the Juncus community were not significantly different between sampling events, indicating there may be a link between the consistently low soil salinity and consistent incorporation of carbon into the soil. This is consistent with results obtained by Kelleway et al., (2016a), where there is more carbon in fluvial settings than in more marine settings. This is also seen in the data from the Melaleuca and Phragmites communities, which have the highest carbon densities, but much lower salinities than the tidal end of the saltmarsh. No analysis of grain size was carried out as a part of this research, hence no relationship can be drawn in this regard, as was done by Kelleway et al., (2016a).

Soil bulk density (BD) does suggest a potential mixed effect on carbon density. A lower BD may be indicative that the carbon stored in a soil will be lower than in a soil with a higher bulk density, due to the open pore spaces and higher surface area that it offers. It could also be indicative of a higher carbon density, as a high percent of OM would take up more volume and contribute to a lower bulk density (Kelleway et al., 2016a; Morris et al., 2016).

In the soil samples obtained during February, the lowest BDs also have the highest OM percentages and are among the higher values for carbon density. These values are summarised in Table 7.3 below. Alternatively, in the May samples, the lowest BDs are again associated with the highest OM percentages, yet this time the lowest organic carbon densities (Table 7.3). Data do not suggest that a higher BD has more potential to preserve carbon. Instead, data are suggestive of OM percentage driving the density of carbon within the soil.

Table 7.3: Summary table showing the Bulk Density (BD), Organic Matter (OM) percentage, and Carbon (C) density values for the vegetation communities in February and May.

		BD (g cm^3)	OM (%)	C Density (g C cm^3)
February	Sarcocornia	N/R	N/R	N/R
	Juncus	0.71 ± 0.02	16.67 ± 0.63	0.0664 ± 0.001
	Melaleuca	0.41 ± 0.09	34.20 ± 6.78	0.0562 ± 0.003
	Phragmites	0.46 ± 0.08	32.36 ± 5.61	0.0637 ± 0.003
May	Sarcocornia	1.06 ± 0.03	10.20 ± 0.33	0.115 ± 0.007
	Juncus	0.53 ± 0.09	22.96 ± 5.51	0.056 ± 0.011
	Melaleuca	0.27 ± 0.03	43.52 ± 5.28	0.035 ± 0.007
	Phragmites	0.32 ± 0.06	30.22 ± 3.42	0.033 ± 0.002

7.3. Site-Wide Estimates of Carbon

A tier one estimate of soil carbon, per the IPCC guidelines outlined by Howard et al., (2014), of carbon stored within the Lake Tilba study site would be the area, 6.9 ha, multiplied by the average for salt marshes, 255 Mg ha^{-1}, resulting in an estimate of 1773 Mg of carbon. This estimation, however, does not factor in varying vegetation types, ground cover, or hydraulic regimes, and as such the true value would be expected to differ greatly. Using site-specific data collection, as done as part of this research project, it would be possible to obtain a value that is more likely to represent the actual situation of the Lake Tilba salt marsh, at least within the uppermost surface layer of the soil. However, the soil sampling carried out as a part of this project only sampled the uppermost 5 cm of soil, due to the shallow sampling depth, results and differences in carbon stocks should only be used to compare differences between marsh zones, not to determine the total carbon pool as this would require much deeper soil sampling and coring (Macreadie, Hughes and Kimbro, 2013). Therefore, no estimate of the site-wide carbon is made based on the measurements made here.

7.4. Limitations and Importance of Research

As mentioned previously, the majority of limitations of this research project arise from not being able to collect additional samples and downloads of data. This is due to the recent lockdown and travel restrictions implemented by the NSW Government in response to the June Coronavirus outbreak. The lack of this data meant that the eddy co-variance data was limited to 42 days, which does not allow for a high temporal resolution to detect both long-term and seasonal trends in GHG emissions. Additionally, part of the original aims of this project was to sample the environmental variables on more than just the two occasions, which may also have allowed for the detection of seasonal changes in variables like soil salinity, biomass and soil carbon. Having access to long-term inundation and

conductivity data from the water loggers would also have allowed for a more in-depth understanding of how inundation and salinity affected CO_2 fluxes from the wetland surface. While the data available as a part of this research project may have been limited, it still provides a starting point into determining how environmental variables interact with one another in the saltmarsh interface, and work to either inhibit or facilitate CO_2 emission and sequestration. Another limitation exists in the calculation of the NEE for the saltmarsh. The value presented in Table 7.1 is likely not a true representation as lateral import and export of carbon both from tidal flows and groundwater transfer have not been taken into consideration during this project, nor is it representative of seasonal trends.

The importance of this project rests in developing an understanding of the relationships between environmental variables such as tidal dynamics, salinity, vegetation characteristics and soil carbon stocks and the effect they have on greenhouse gas emissions. This is an important starting point for factoring saltmarsh and other coastal wetland ecosystems into blue carbon accounting frameworks and coastal management initiatives. Furthermore, this understanding can facilitate more efficient strategies to conserve and restore coastal wetlands to protect biodiversity, coastal communities and mitigate anthropogenic emissions exacerbating global warming.

8. Conclusion

Measurement of CO_2 fluxes from the two vegetation communities in the Lake Tilba saltmarsh revealed that there was a significant difference in the between the fluxes of the two communities. The community dominated by *J. kraussii* had a more negative flux, both when comparing the daily averaged half-hour flux, and that daily average daytime half-hourly flux. Additionally, this community had higher biomass, and an overall higher sequestration capacity. Biomass productivity may be the primary driver of the difference in fluxes between the two vegetation communities. Additionally, soil and groundwater salinity data indicate that a freshwater lens occurring beneath the Juncus community may be controlling the vegetative productivity and subsequent sequestration capacity of the Juncus community. This lens may also be contributing to reduced salinities seen in the Melaleuca and Phragmites communities and allowing for higher carbon densities to arise. Trends also arose in bulk density, with a decrease towards to land-ward end of the established transect. Organic matter proportion may be an explaining variable for bulk density; however, more analysis of this relationship in necessary before this conclusion can be properly drawn.

While the Lake Tilba saltmarsh is small in comparison to other NSW South Coast sites, it can still provide a starting point for assessing how CO_2 fluxes can vary between vegetation communities, what driving variables may be responsible for these differences and how NSW estuaries may respond to the challenges of sea-level rise. It is recommended then, that more monitoring and sampling of the site is carried out, to develop a more complete idea of the interactions occurring here over longer temporal scales, and how findings may be applied to areas outside of the Lake Tilba saltmarsh. Furthermore, the addition of CH_4 sensors would allow an idea to be formed at how the saltmarsh is acting as either a sink or source for greenhouse gasses overall.

9. References

Abdul-Aziz, O.I. et al. (2018) "Environmental Controls, Emergent Scaling, and Predictions of Greenhouse Gas (GHG) Fluxes in Coastal Salt Marshes," Journal of Geophysical Research: Biogeosciences, 123(7). doi:10.1029/2018JG004556.

Aubinet, M., Vesala, T. and Papale, D. (2012) Eddy Covariance: A Practical Guide to Measurement and Data Analysis.

Ball, B.C. (2013) "Soil structure and greenhouse gas emissions: A synthesis of 20 years of experimentation," European Journal of Soil Science, 64(3), pp. 357–373. doi:10.1111/ejss.12013.

Bange, H.W. (2006) "Nitrous oxide and methane in European coastal waters," Estuarine, Coastal and Shelf Science, 70(3), pp. 361–374. doi:10.1016/j.ecss.2006.05.042.

Brown, D.R. et al. (2021) "Hypersaline tidal flats as important 'blue carbon' systems: a case study from three ecosystems," Biogeosciences, 18(8). doi:10.5194/bg-18-2527-2021.

Burba, G. and Anderson, D. (2010) A Brief Practical Guide to Eddy Covariance Flux Measurements: Principles and Workflow Examples for Scientific and Industrial Applications. LI-COR Biosciences.

Byrd, K.B. et al. (2018) "A remote sensing-based model of tidal marsh aboveground carbon stocks for the conterminous United States," ISPRS Journal of Photogrammetry and Remote Sensing, 139, pp. 255–271. doi:10.1016/j.isprsjprs.2018.03.019.

Campbell Scientific (2020) "EASYFLUX DL CR6OP For CR6 and Open-Path Eddy-Covariance System."

Carslaw, D.C. and Ropkins, K. (2012) "openair — An R package for air quality data analysis," Environmental Modelling & Software, 27–28. doi:10.1016/j.envsoft.2011.09.008.

Chambers, L.G., Reddy, K.R. and Osborne, T.Z. (2011) "Short-Term Response of Carbon Cycling to Salinity Pulses in a Freshwater Wetland," Soil Science Society of America Journal, 75(5). doi:10.2136/sssaj2011.0026.

Chojnicki, B.H., Acosta, M. and Augustin, J. (2014) Measurements of Carbon Dioxide Fluxes by Chamber Method at the Rzecin Wetland Ecosystem, Poland. Available at: https://www.researchgate.net/publication/233990948.

Clarke, P. and Jacoby, C. (1994) "Biomass and above-ground productivity of salt-marsh plants in south-eastern Australia," Marine and Freshwater Research, 45(8). doi:10.1071/MF9941521.

Craft, C.B. (2012) "Tidal freshwater forest accretion does not keep pace with sea level rise," Global Change Biology, 18(12). doi:10.1111/gcb.12009.

Craft, C.B., Seneca, E.D. and Broome, S.W. (1991) "Loss on ignition and kjeldahl digestion for estimating organic carbon and total nitrogen in estuarine marsh soils: Calibration with dry combustion," Estuaries, 14(2), pp. 175–179. doi:10.2307/1351691.

Crooks, S. et al. (2011) Marine Ecosystem Series Mitigating Climate Change through Restoration and Management of Coastal Wetlands and Near-shore Marine Ecosystems Challenges and Opportunities. Available at: www.worldbank.org/environment/publications.

Department of the Environment and Energy (2016) Coastal Wetlands - Mangroves and Saltmarshes. Available at: www.dpi.

Donato, D.C. et al. (2011) "Mangroves among the most carbon-rich forests in the tropics," Nature Geoscience, 4(5). doi:10.1038/ngeo1123.

Dondini, M. et al. (2018) "Projecting Soil C Under Future Climate and Land-Use Scenarios (Modeling)," in Soil Carbon Storage. Elsevier. doi:10.1016/B978-0-12-812766-7.00009-3.

Doroski, A.A., Helton, A.M. and Vadas, T.M. (2019) "Greenhouse gas fluxes from coastal wetlands at the intersection of urban pollution and saltwater intrusion: A soil core experiment," Soil Biology and Biochemistry, 131, pp. 44–53. doi:10.1016/j.soilbio.2018.12.023.

Drexler, J.Z. et al. (2004) "A review of models and micrometeorological methods used to estimate wetland evapotranspiration," Hydrological Processes, 18(11), pp. 2071–2101. doi:10.1002/hyp.1462.

Emery, H.E. et al. (2021) "Tidal rewetting in salt marshes triggers pulses of nitrous oxide emissions but slows carbon dioxide emission," Soil Biology and Biochemistry, 156. doi:10.1016/j.soilbio.2021.108197.

Emery, H.E. and Fulweiler, R.W. (2014) "Spartina alterniflora and invasive Phragmites australis stands have similar greenhouse gas emissions in a New England marsh," Aquatic Botany, 116, pp. 83–92. doi:10.1016/j.aquabot.2014.01.010.

Foken, T. et al. (2012) "Corrections and Data Quality Control," in Eddy Covariance. Springer Netherlands, pp. 85–131. doi:10.1007/978-94-007-2351-1_4.

Forbrich, I., Giblin, A.E. and Hopkinson, C.S. (2018) "Constraining Marsh Carbon Budgets Using Long-Term C Burial and Contemporary Atmospheric CO 2 Fluxes," Journal of Geophysical Research: Biogeosciences, 123(3). doi:10.1002/2017JG004336.

Gorham, C. et al. (2021) "Soil Carbon Stocks Vary Across Geomorphic Settings in Australian Temperate Tidal Marsh Ecosystems," Ecosystems, 24(2). doi:10.1007/s10021-020-00520-9.

Hedges, J.I. and Keil, R.G. (1995) "Sedimentary organic matter preservation: an assessment and speculative synthesis," Marine Chemistry, 49(2–3). doi:10.1016/0304-4203(95)00008-F.

Heiri, O., Lotter, A.F. and Lemcke, G. (2001) "Loss on ignition as a method for estimating organic and carbonate content in sediments: reproducibility and comparability of results," Journal of Paleolimnology, 25(1). doi:10.1023/A:1008119611481.

Howard, J., et al. (2014) COASTAL BLUE CARBON methods for assessing carbon stocks and emissions factors in mangroves, tidal salt marshes, and seagrass meadows. Arlington. Available at: www.ioc.unesco.org.

Hughes, M.G., Rogers, K. and Wen, L. (2019) "Saline wetland extents and tidal inundation regimes on a micro-tidal coast, New South Wales, Australia," Estuarine, Coastal and Shelf Science, 227. doi:10.1016/j.ecss.2019.106297.

Hyndes, G.A. et al. (2014) "Mechanisms and ecological role of carbon transfer within coastal seascapes," Biological Reviews, 89(1), pp. 232–254. doi:10.1111/brv.12055.

IPCC (2007) Climate Change 2007: Synthesis Report. Contribution of Working Groups I, II and III to the Fourth Assessment Report of the Intergovernmental Panel on Climate Change. Geneva.

Kelleway, J.J., Saintilan, N., Macreadie, P.I. and Ralph, P.J. (2016) (*Kelleway et al., 2016a*) "Sedimentary Factors are Key Predictors of Carbon Storage in SE Australian Saltmarshes," *Ecosystems*, 19(5), pp. 865–880. doi:10.1007/s10021-016-9972-3.

Kelleway, J.J., Saintilan, N., Macreadie, P.I., Skilbeck, C.G., *Zawadzki, A., Ralph, P.J.,* (2016) (Kelleway et al., 2016b) "Seventy years of continuous encroachment substantially increases 'blue carbon' capacity as mangroves replace intertidal salt marshes," *Global Change Biology*, 22(3). doi:10.1111/gcb.13158.

Kelleway, J.J. et al. (2017) "Sediment and carbon deposition vary among vegetation assemblages in a coastal salt marsh," Biogeosciences, 14(16), pp. 3763–3779. doi:10.5194/bg-14-3763-2017.

Krauss, K.W. et al. (2018) "The Role of the Upper Tidal Estuary in Wetland Blue Carbon Storage and Flux," Global Biogeochemical Cycles, 32(5), pp. 817–839. doi:10.1029/2018GB005897.

Kristensen, E. et al. (2017) "Biogeochemical Cycles: Global Approaches and Perspectives," in Mangrove Ecosystems: A Global Biogeographic Perspective. Cham: Springer International Publishing. doi:10.1007/978-3-319-62206-4_6.

Lill, A.W.T. et al. (2013) "Isolation and connectivity: Relationships between periodic connection to the ocean and environmental variables in intermittently closed estuaries," Estuarine, Coastal and Shelf Science, 128. doi:10.1016/j.ecss.2013.05.011.

Livesley, S.J. and Andrusiak, S.M. (2012) "Temperate mangrove and salt marsh sediments are a small methane and nitrous oxide source but important carbon store," Estuarine, Coastal and Shelf Science, 97, pp. 19–27. doi:10.1016/j.ecss.2011.11.002.

Loomis, M.J. and Craft, C.B. (2010) "Carbon Sequestration and Nutrient (Nitrogen, Phosphorus) Accumulation in River-Dominated Tidal Marshes, Georgia, USA," Soil Science Society of America Journal, 74(3). doi:10.2136/sssaj2009.0171.

Lovelock, C.E. et al. (2014) "Contemporary Rates of Carbon Sequestration Through Vertical Accretion of Sediments in Mangrove Forests and Saltmarshes of South East Queensland, Australia," Estuaries and Coasts, 37(3). doi:10.1007/s12237-013-9702-4.

Luo, M. et al. (2019) "Impacts of increasing salinity and inundation on rates and pathways of organic carbon mineralization in tidal wetlands: a review," Hydrobiologia. Springer International Publishing, pp. 31–49. doi:10.1007/s10750-017-3416-8.

Macreadie, P.I. et al. (2017) "Carbon sequestration by Australian tidal marshes," Scientific Reports, 7(1). doi:10.1038/srep44071.

Macreadie, P.I., Hughes, A.R. and Kimbro, D.L. (2013) "Loss of 'Blue Carbon' from Coastal Salt Marshes Following Habitat Disturbance," PLoS ONE, 8(7). doi:10.1371/journal.pone.0069244.

Mendes, K.R. et al. (2020) "Seasonal variation in net ecosystem CO_2 exchange of a Brazilian seasonally dry tropical forest," Scientific Reports, 10(1). doi:10.1038/s41598-020-66415-w.

Mills, K. (2021) ILLAWARRA VEGETATION STUDIES OCCASIONAL PAPERS ON THE VEGETATION OF THE ILLAWARRA AND SOUTH COAST REGIONS.

Morris, J.T. et al. (2016) "Contributions of organic and inorganic matter to sediment volume and accretion in tidal wetlands at steady state," Earth's Future, 4(4). doi:10.1002/2015EF000334.

Moseman-Valtierra, S. et al. (2016) "Carbon dioxide fluxes reflect plant zonation and belowground biomass in a coastal Marsh," Ecosphere, 7(11). doi:10.1002/ecs2.1560.

Naidoo, G. and Kift, J. (2006) "Responses of the saltmarsh rush Juncus kraussii to salinity and waterlogging," Aquatic Botany, 84(3). doi:10.1016/j.aquabot.2005.10.002.

Negandhi, K. et al. (2019) "Blue carbon potential of coastal wetland restoration varies with inundation and rainfall," Scientific Reports, 9(1). doi:10.1038/s41598-019-40763-8.

NSW Government (2021) Coastal Saltmarsh in the New South Wales North Coast, Sydney Basin and South East Corner Bioregions - profile.

Oppenheimer, M. et al. (2019) Sea Level Rise and Implications for Low-Lying Islands, Coasts and Communities. Poh Poh Wong.

Owers, C.J., Rogers, K. and Woodroffe, C.D. (2018) "Terrestrial laser scanning to quantify above-ground biomass of structurally complex coastal wetland vegetation," Estuarine, Coastal and Shelf Science, 204. doi:10.1016/j.ecss.2018.02.027.

Peichl, M. et al. (2014) "A 12-year record reveals pre-growing season temperature and water table level threshold effects on the net carbon dioxide exchange in a boreal fen," Environmental Research Letters, 9(5). doi:10.1088/1748-9326/9/5/055006.

Reichle, D.E. (2020) "Energy flow in ecosystems," in The Global Carbon Cycle and Climate Change. Elsevier. doi:10.1016/B978-0-12-820244-9.00008-1.

Reichstein, M. et al. (2005) "On the separation of net ecosystem exchange into assimilation and ecosystem respiration: review and improved algorithm," Global Change Biology, 11(9). doi:10.1111/j.1365-2486.2005.001002.x.

Restaino, J.C. and Peterson, D.L. (2013) "Wildfire and fuel treatment effects on forest carbon dynamics in the western United States," Forest Ecology and Management, 303. doi:10.1016/j.foreco.2013.03.043.

Rogers, K. et al. (2019) "Blue carbon in coastal landscapes: a spatial framework for assessment of stocks and additionality," Sustainability Science, 14(2), pp. 453–467. doi:10.1007/s11625-018-0575-0.

Rosentreter, J.A. et al. (2021) "Methane and Nitrous Oxide Emissions Complicate Coastal Blue Carbon Assessments," Global Biogeochemical Cycles. Blackwell Publishing Ltd. doi:10.1029/2020GB006858.

Roy, P.S. et al. (2001) "Structure and function of south-east Australian estuaries," Estuarine, Coastal and Shelf Science, 53(3), pp. 351–384. doi:10.1006/ecss.2001.0796.

Saintilan, N. (2009) Australian Saltmarsh Ecology. Edited by N. Saintilan. CSIRO Publishing.

Saintilan, N. et al. (2013) "Allochthonous and autochthonous contributions to carbon accumulation and carbon store in southeastern Australian coastal wetlands," Estuarine, Coastal and Shelf Science, 128. doi:10.1016/j.ecss.2013.05.010.

Saintilan, N. et al. (2019) "Climate Change Impacts on the Coastal Wetlands of Australia," Wetlands. Springer, pp. 1145–1154. doi:10.1007/s13157-018-1016-7.

Singh, N. et al. (2019) "Net Ecosystem Exchange of CO2 in Deciduous Pine Forest of Lower Western Himalaya, India," Resources, 8(2). doi:10.3390/resources8020098.

Spalding, M.D. et al. (2014) "The role of ecosystems in coastal protection: Adapting to climate change and coastal hazards," Ocean and Coastal Management, 90, pp. 50–57. doi:10.1016/j.ocecoaman.2013.09.007.

Wickland, K.P. and Neff, J.C. (2008) "Decomposition of soil organic matter from boreal black spruce forest: environmental and chemical controls," Biogeochemistry, 87(1). doi:10.1007/s10533-007-9166-3.

Yin, S. et al. (2019) "Effects of soil moisture on carbon mineralization in floodplain wetlands with different flooding frequencies," Journal of Hydrology, 574. doi:10.1016/j.jhydrol.2019.05.007.

Zhou, L. et al. (2015) "Spartina alterniflora Invasion Alters Carbon Exchange and Soil Organic Carbon in Eastern Salt Marsh of China," CLEAN - Soil, Air, Water, 43(4). doi:10.1002/clen.201300838.
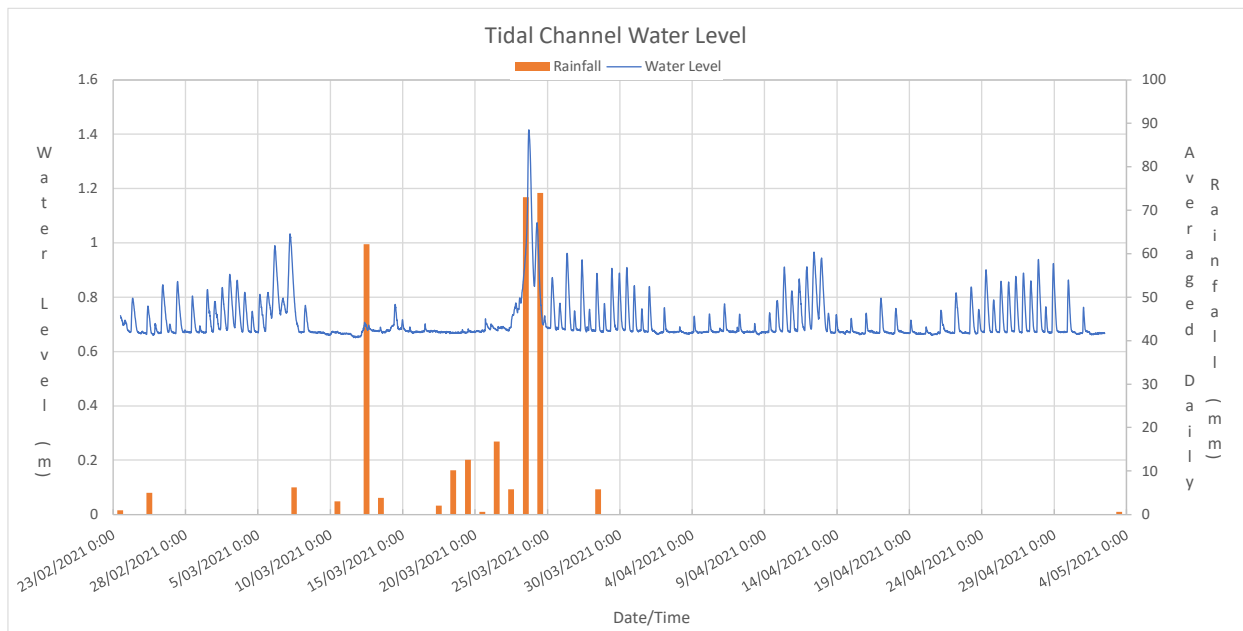
10. Appendix

Figure 10.9.1:Water logger data from the tidal channel logger. Water level and daily rainfall data from Narooma are plotted together against time. Water level has been adjusted to show level relative to Australian Height Datum (AHD).
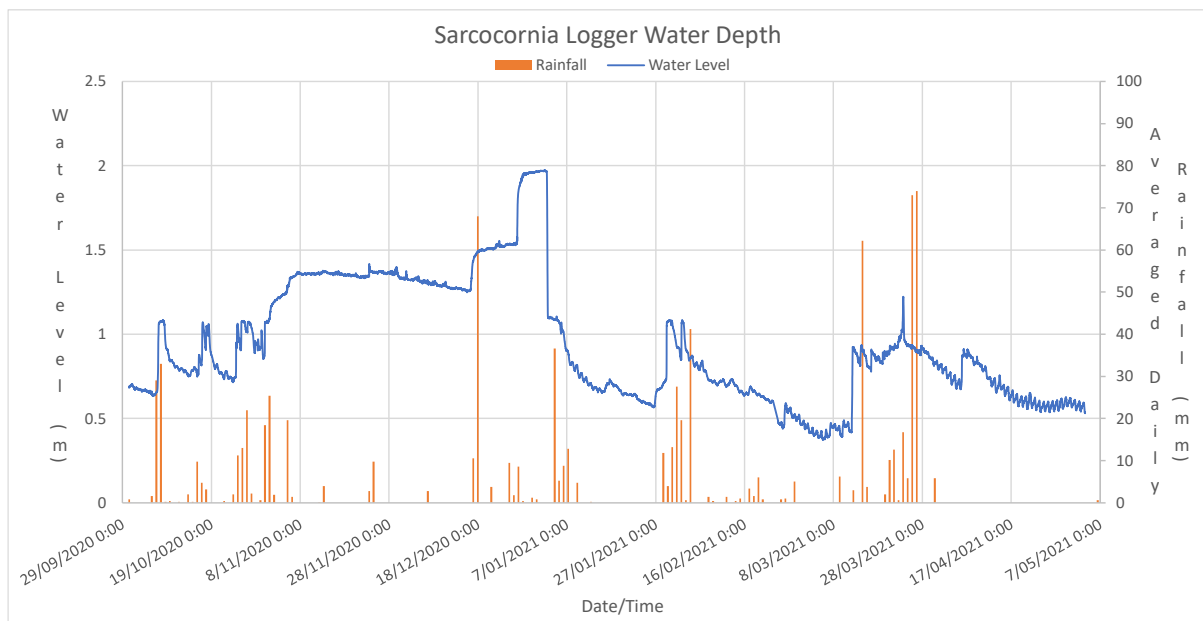

Figure 10.2:Water logger data from the Sarcocornia community. Water level and daily rainfall data from Narooma are plotted together against time. Water level has been adjusted to show level relative to Australian Height Datum (AHD).
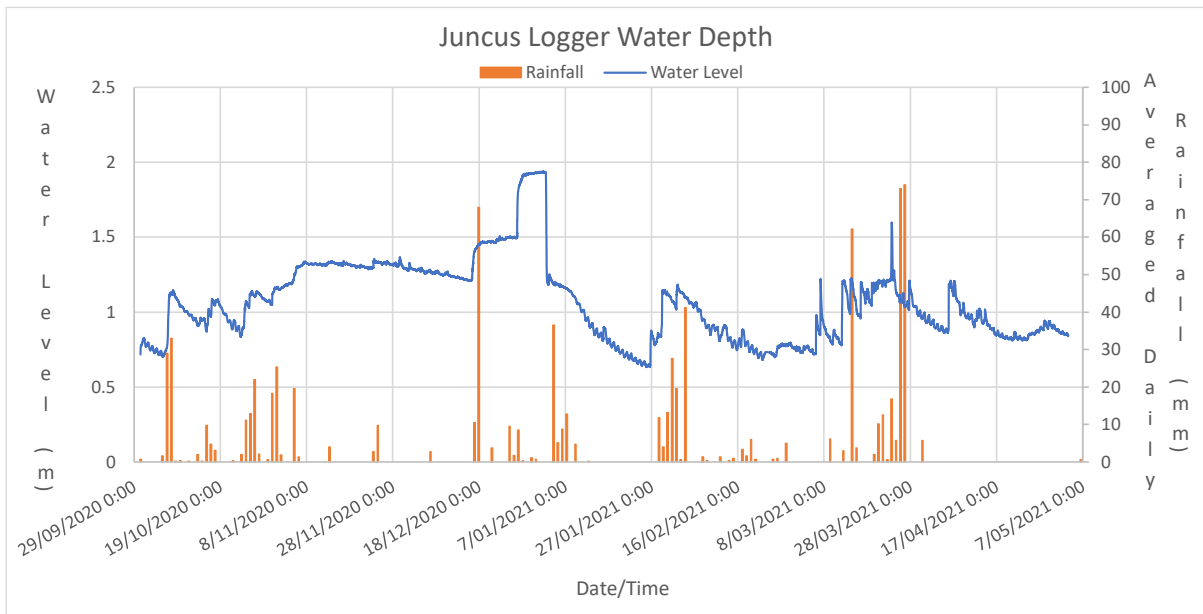
64

Figure 10.3: Water logger data from the Juncus community. Water level and daily rainfall data from Narooma are plotted together against time. Water level has been adjusted to show level relative to Australian Height Datum (AHD).
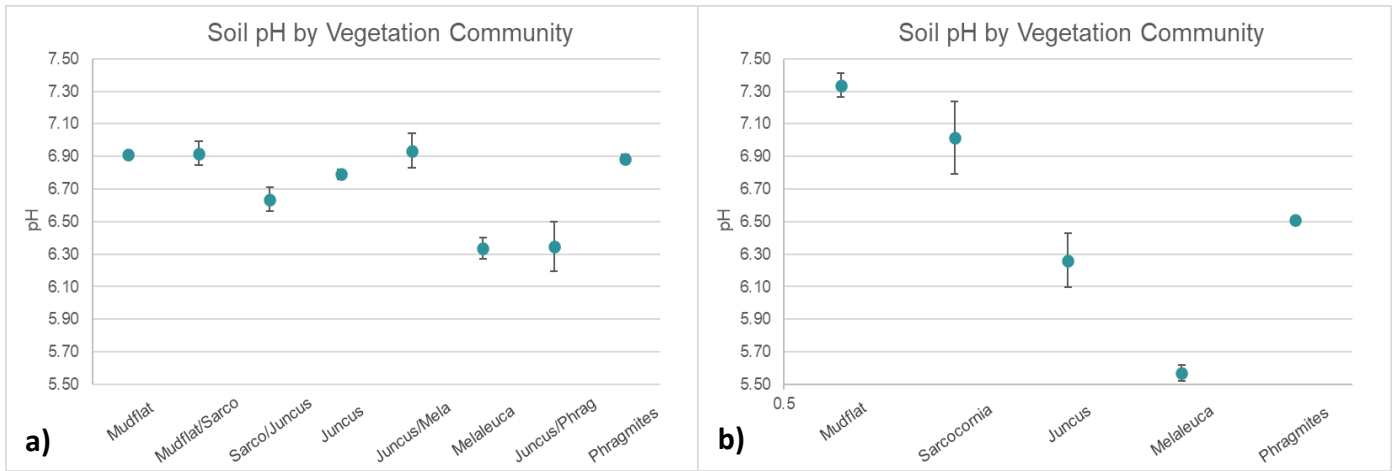

Figure 10.4:Soil pH for each vegetation community for a) February, and b) May. Values are averages and the error bars represent ± standard error.
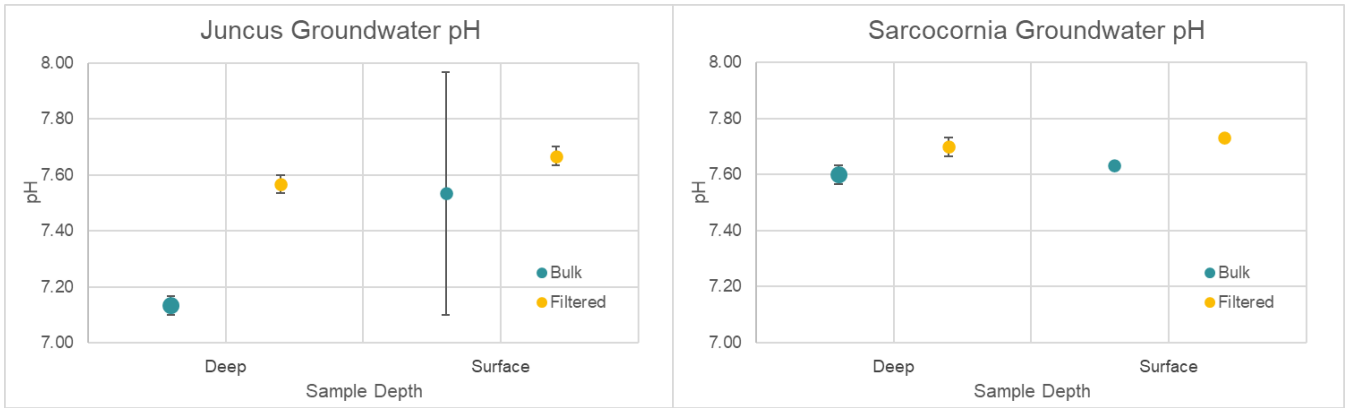
Figure 10.5:Juncus and Sarcocornia community groundwater pH results from the February. Data points are averages of three replicates per sampling treatment. Error bars represent standard error
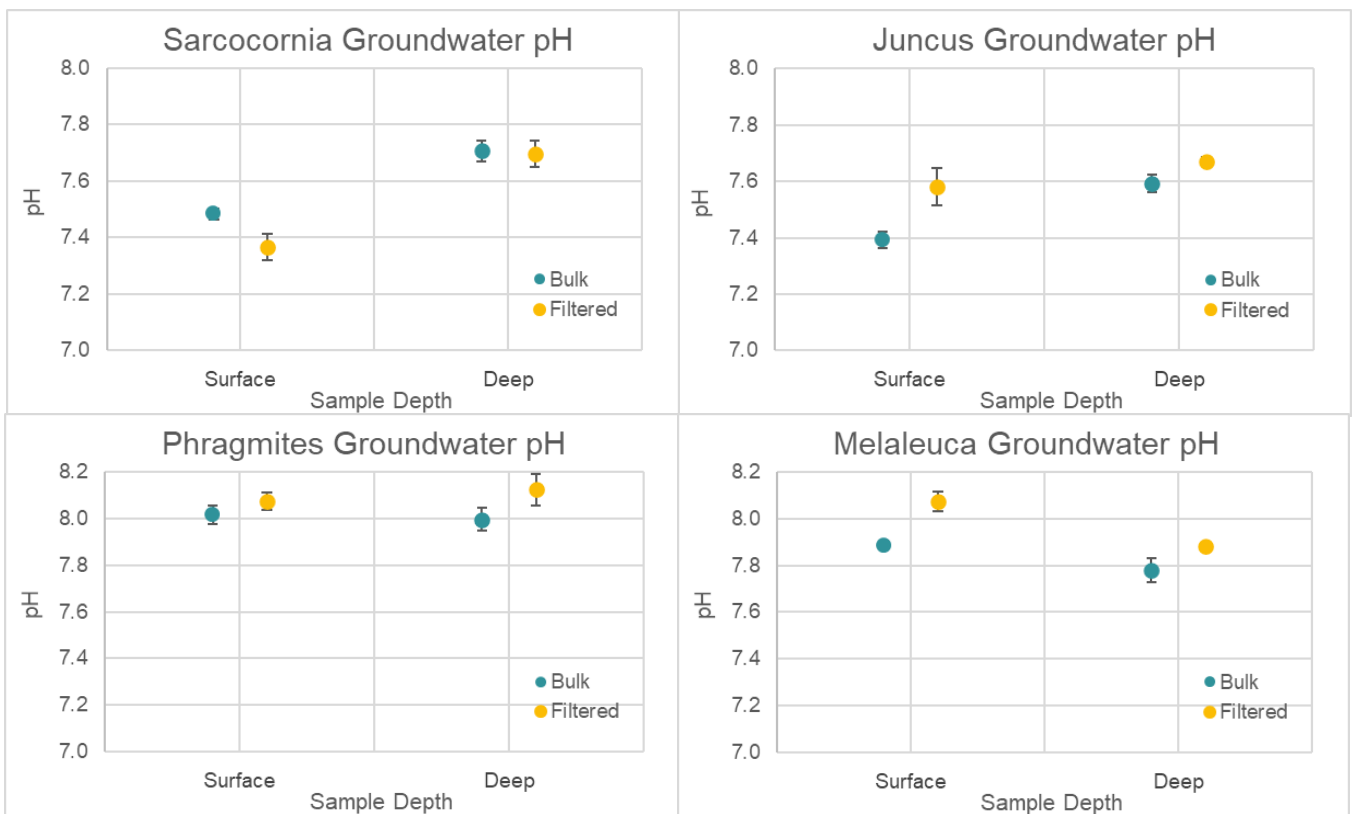

Figure 10.6:Community groundwater pH results from all four standpipes for May. Data points are averages of three replicates per sampling treatment. Error bars represent standard error.

Table 10.1:Replicate data for each biomass sample conducted across the Lake Tilba Saltmarsh

| Replicate #	Species	Total Wet Weight (g)	Total Dry Weight (g)	MC%	BM%	kg dry/m²	%Veg dry by Weight
Sarcocornia 1	Sarcocornia quinqueflora	682.77	133.76	80.4	19.6	0.54	100
Sarcocornia 2	Sarcocornia quinqueflora	438.14	91.43	79.1	20.9	0.37	100
Sarcocornia 3	Sarcocornia quinqueflora	689.25	134.59	80.5	19.5	0.54	100
					Mean	0.48	
Juncus 1	Juncus kraussii	1141.91	417.17	63.5	36.5	1.67	80.3
	Sarcocornia quinqueflora	510.92	64.02	87.5	12.5	0.26	12.3
	Paspaylum distichum	94.3	31.04	67.1	32.9	0.12	6.0
	Samolus repens	48.83	7.12	85.4	14.6	0.03	1.4
	TOTAL	1795.96	519.35	71.1	28.9	2.08	
Juncus 2	Juncus kraussii	69.33	23.51	66.1	33.9	0.09	10.5
	Sarcocornia quinqueflora	1366.13	198.68	85.5	14.5	0.79	88.4
	Paspaylum distichum	0	0	0.0	0.0	0.00	0.0
	Samolus repens	7.86	1.37	82.6	17.4	0.01	0.6
	Trigloghin striatum	8.28	1.12	86.5	13.5	0.004	0.5
	TOTAL	1451.6	224.68	84.5	15.5	0.90	
Juncus 3	Juncus kraussii	214.77	76.45	64.4	35.6	0.31	31.6
	Sarcocornia quinqueflora	1060.07	165.42	84.4	15.6	0.66	68.4
	Samolus repens	0.95	0.14	85.5	14.5	0.001	0.1
	TOTAL	1275.79	242.01	81.0	19.0	0.97	
Phragmites 1	Phragmites australis	310.88	84.09	73.0	27.0	0.34	33.8
	Juncus kraussii	347.33	104.12	70.0	30.0	0.42	41.8
	Sarcocornia quinqueflora	319.74	51.66	83.8	16.2	0.21	20.7
	Samolus repens	52.94	9.26	82.5	17.5	0.04	3.7
	TOTAL	1030.89	249.13	75.8	24.2	1.00	
Phragmites 2	Phragmites australis	766.14	166.05	78.3	21.7	0.66	73.3
	Juncus kraussii	37.94	6.70	82.3	17.7	0.03	3.0
	Sarcocornia quinqueflora	11.71	1.70	85.5	14.5	0.01	0.8
	Samolus repens	418.45	52.05	87.6	12.4	0.21	23.0
	TOTAL	1234.24	226.50	81.6	18.4	0.91	
Phragmites 3	Phragmites australis	761.35	229.02	69.9	30.1	0.92	86.4
	Juncus kraussii	125.16	33.40	73.3	26.7	0.13	12.6
	Sarcocornia quinqueflora	2.80	0.35	87.5	12.5	0.00	0.1
	Samolus repens	11.92	2.25	81.1	18.9	0.01	0.8
	TOTAL	901.23	265.02	70.6	29.4	1.06	
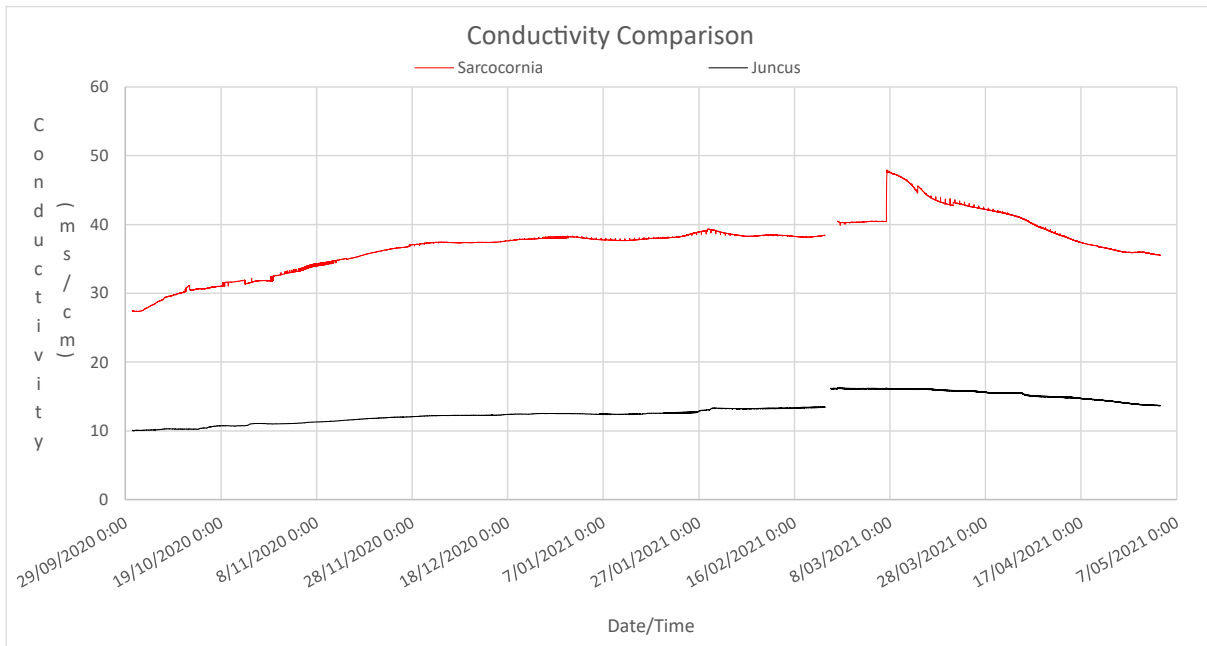
Figure 10.7: Conductivity data from the Sarcocornia and Juncus community's water loggers. Data has been removed for the period of time when loggers were taken from the standpipes so as to not show the effects of disturbance